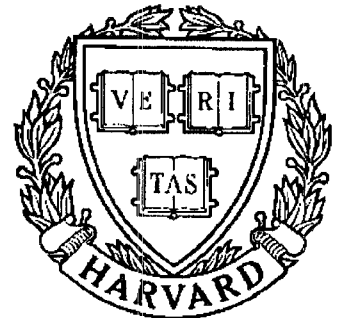


TECHNICAL RESEARCH REPORT



S Y S T E M S
R E S E A R C H
C E N T E R



*Supported by the
National Science Foundation
Engineering Research Center
Program (NSFD CD 8803012),
Industry and the University*

On the Geometry and Dynamics of Floating Four-Bar Linkages

by R. Yang and P.S. Krishnaprasad

ON THE GEOMETRY AND DYNAMICS
OF FLOATING FOUR-BAR LINKAGES *

Rui Yang

P. S. Krishnaprasad

Electrical Engineering Department
&
Systems Research Center
University of Maryland, College Park.

ABSTRACT

In this paper, we investigate the kinematics and dynamics of *floating*, planar four-bar linkages. The geometry of configuration space is analyzed through the classical theory of mechanisms due to Grashof. The techniques of symplectic and Poisson reduction are used to understand the dynamics of the system. Bifurcations of relative equilibria for linkages admitting symmetric shapes are studied using the techniques of singularity theory. The problem of reconstruction of the full dynamics and its relation to geometric phases is discussed through some examples. This research reveals that a coupled mechanical system with kinematic loops possesses richer and more complicated dynamical aspects in comparison with systems which have the same number of degrees of freedom, but no kinematic loops.

* This work was supported in part by the AFOSR University Research Initiative Program under grant AFOSR-90-0105 and by the National Science Foundation's Engineering Research Centers Program: NSFD CDR 8803012.

1. INTRODUCTION

There has been significant progress in our understanding of the hamiltonian structure of serial-link (or open chain) multibody systems (Baillieul [1988]; Baillieul & Levi [1987]; Grossman, Krishnaprasad & Marsden [1988]; Krishnaprasad & Marsden [1987]; Marsden, Krishnaprasad & Simo [1988]; Oh et al. [1989]; Posbergh [1988]; Posbergh, Krishnaprasad & Marsden [1987]; Simo, Marsden & Krishnaprasad [1988]; Simo, Posbergh & Marsden [1989]; Sreenath [1987]; Sreenath et al. [1988]; Wang & Krishnaprasad [1989]). The application of geometric methods, symmetry principles and reduction has led to deeper knowledge of the dynamics of model problems. This insight has also been helpful in developing appropriate control-theoretic tools (Bloch, Reyhanoglu & McClamroch [1991]; Krishnaprasad & Yang [1991]; Sreenath [1990]). The primary source of motivation for such problems has been in aerospace engineering where imaginative designs of multibody spacecraft have been proposed and on occasion realized (Bianchi & Schielen [1985]; CIME [1972]; Wittenburg [1977]).

On the other hand, problems in aerospace engineering also suggest that multibody systems with kinematic loops are of practical importance. An important example may be the parallel linkage based robot manipulators which have been contemplated for space applications. However, as we shall see, the presence of loop closure constraints implies that the knowledge of hamiltonian structure and phase portraits for open chain multibody systems cannot be applied directly to systems with closed loops. For instance, for multibody systems with closed loops, the topological description of configuration space strongly depends on the choice of kinematic parameters. This is not true for systems with open chains.

In this paper, we study the kinematics and dynamics of the simplest mechanical system with a kinematic loop — the planar, *floating* four-bar linkage. By *floating* we mean that no link is fixed in space. It is simplest in that it has the fewest degrees of freedom (after symmetry reduction) among all kinds of mechanisms with closed loops. In the theory of machines, the four-bar linkage (with one link, the *frame*, fixed) plays an extremely important role (Hunt [1978]). It may be directly used in many mechanical systems. More complex mechanisms are often synthesized using one four-bar linkage to

drive another. It is of further interest that a four-bar linkage can generate the wide variety of motions which are represented by *coupler curves* (Hrones & Nelson [1951]). For floating four-bar linkages, one expects similar properties to hold. As we shall show in this paper, floating four-bar linkages do possess very interesting features from both kinematic and dynamic points of view.

The outline of this paper is as follows. After stating the basic notations for this paper in section 2, we give a geometric description of the configuration space in section 3. In section 4, we give an explicit expression for the kinetic energy which is also the lagrangian since in this paper we assume that no potential energy is involved. From this section we see that explicit computation of constrained dynamics is difficult. Yet in the present setting, using geometric techniques, one can infer qualitative properties without recourse to explicit analytic representation of the constrained dynamics. This we do in section 5, wherein we explore symmetry properties, hamiltonian structure and reduction of four bar linkage dynamics. In section 6 we use a theorem of Smale to compute relative equilibria for the dynamics of a four-bar linkage. Further, using techniques from singularity theory, we study the local bifurcations of relative equilibria for linkages which admit symmetric shapes. In section 7, the phase reconstruction problem for a four-bar linkage is investigated. It is interesting to note that it is possible to generate either positive or negative phase shift by the motion in shape space. This phenomenon does not arise in a planar two-body system which also has two degrees of freedom.

Preliminary versions of this paper were presented at the IEEE Conference on Decision and Control (Yang & Krishnaprasad [1989]; Yang & Krishnaprasad [1990]).

We are pleased to acknowledge useful discussions on the topics of this paper with Jerrold Marsden and Tim Healey.

2. NOTATIONS AND GEOMETRIC CONSTRAINTS

The structure of a closed floating four-bar linkage is represented in Figure 2.1. What we mean by *bar* in this paper is a planar rigid body, on which the center of mass and pin joints are located arbitrarily. The bars are labeled sequentially from 0 to 3. On each bar, a body-fixed frame is attached such that its origin is at the center of mass of the bar and the x -axis is parallel to the line connecting two joints on the bar. In particular, we choose the positive direction of x -axis of i -th bar towards the $(i + 1)$ -th bar, for $i = 0, 1, 2, 3 \pmod{4}$. We define the following quantities.

\mathbf{d}_{ij}	the vector from the center of mass of i -th bar to the joint with j -th bar in body-fixed frame;
\mathbf{r}_i	the position vector of the center of mass of i -th bar relative to an inertial observer;
\mathbf{r}_i^c	the vector from the system center of mass to the center of mass of i -th bar;
\mathbf{r}_c	the position of the system center of mass relative to the reference point of the inertial observer;
θ_i	the orientation angle of i -th bar relative to the inertial frame;
θ_{ij}	the relative angle between i -th bar and j -th bar, i.e., $\theta_{ij} = \theta_i - \theta_j$;
l_i	the <i>length</i> of i -th bar, which is defined as the distance between the joints on i -th bar, i.e. $l_i = \ \mathbf{d}_{i,i+1} - \mathbf{d}_{i,i-1}\ $;
m_i, I_i	the mass and the moment of inertia of i -th bar about its center of mass;
m	the total mass of the system, i.e.

$$m = \sum_{i=0}^3 m_i.$$

Any pair of adjacent bodies is connected by the following relation, *the hinge*

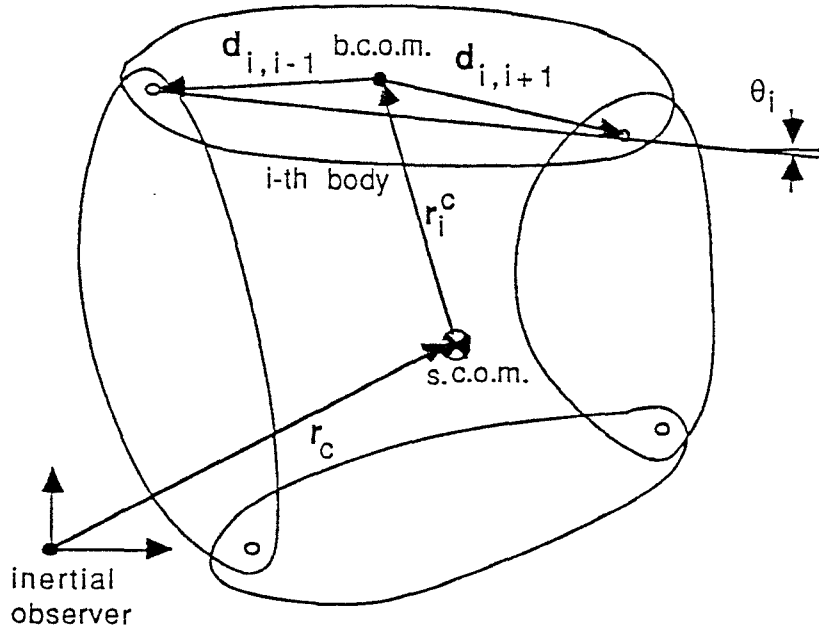


Figure 2.1 The general structure of four-bar linkage

constraint,

$$\mathbf{r}_{i+1}^c = \mathbf{r}_i^c + R(\theta_i)\mathbf{d}_{i,i+1} - R(\theta_{i+1})\mathbf{d}_{i+1,i} \quad i = 0, 1, 2, 3 \pmod{4}. \quad (2.1)$$

where

$$R(\theta_i) = \begin{pmatrix} \cos(\theta_i) & -\sin(\theta_i) \\ \sin(\theta_i) & \cos(\theta_i) \end{pmatrix}$$

the rotation matrix. By eliminating \mathbf{r}_i^c in (2.1) we find the loop constraint or *closure constraint,*

$$\sum_{i=0}^3 R(\theta_i)(\mathbf{d}_{i,i+1} - \mathbf{d}_{i+1,i}) = 0, \quad (2.2)$$

where the convention of modulo 4 for the subscripts is adopted.

3. THE CONFIGURATION SPACE

In this section we investigate the conditions under which the loop constraint (2.2) describes a submanifold of the configuration manifold of an open four-bar chain.

For a planar floating four-bar *open* chain, the configuration space is

$$M = R^2 \times S^1 \times S^1 \times S^1 \times S^1.$$

Here M is a 6-dimensional smooth manifold with local coordinates

$$\mathbf{q} = (x_0, y_0, \theta_0, \theta_1, \theta_2, \theta_3).$$

This corresponds to keeping track of a material point (say center of mass on one of the bodies) and the four absolute orientations. See (Oh et al. [1989]; Sreenath [1987]; Sreenath et al. [1988]) for the hamiltonian mechanics of such open chains.

For a *closed* four-bar mechanism considered in this paper, the configuration space denoted by Q is a subset of M determined by (2.2), i.e.

$$Q = \{\mathbf{q} \in M | \mathbf{F}(\mathbf{q}) = \mathbf{0}\}$$

for

$$\mathbf{F}(\mathbf{q}) = \sum_{i=0}^3 R(\theta_i)(\mathbf{d}_{i,i+1} - \mathbf{d}_{i,i-1}). \quad (3.1)$$

For Q to be a submanifold of M , we have the following condition.

Theorem 3.1: If

$$l_0 \pm l_1 \pm l_2 \pm l_3 \neq 0,$$

Q is a submanifold of M .

Proof: Note that $\mathbf{F} : M \rightarrow R^2$. From (Guillemin & Pollack [1974]) we know that if $\mathbf{0}$ is a regular value of \mathbf{F} , i.e. $\partial\mathbf{F}/\partial\mathbf{q}$ has full rank for all $\mathbf{q} \in Q$, then Q is a submanifold of M .

From (3.1) we have

$$\frac{\partial\mathbf{F}}{\partial\mathbf{q}} = \begin{pmatrix} 0 & 0 & -l_0 \sin(\theta_0) & -l_1 \sin(\theta_1) & -l_2 \sin(\theta_2) & -l_3 \sin(\theta_3) \\ 0 & 0 & l_0 \cos(\theta_0) & l_1 \cos(\theta_1) & l_2 \cos(\theta_2) & l_3 \cos(\theta_3) \end{pmatrix}.$$

It is easy to check that all the nontrivial determinants of 2×2 submatrices are given by the following functions,

$$\begin{aligned}
g_1(\mathbf{q}) &= l_0 l_1 \sin(\theta_1 - \theta_0) \\
g_2(\mathbf{q}) &= l_0 l_2 \sin(\theta_2 - \theta_0) \\
g_3(\mathbf{q}) &= l_0 l_3 \sin(\theta_3 - \theta_0) \\
g_4(\mathbf{q}) &= l_1 l_2 \sin(\theta_2 - \theta_1) \\
g_5(\mathbf{q}) &= l_1 l_3 \sin(\theta_3 - \theta_1) \\
g_6(\mathbf{q}) &= l_2 l_3 \sin(\theta_3 - \theta_2).
\end{aligned} \tag{3.2}$$

Therefore, if for each $\mathbf{q} \in Q$, there exists an i such that $g_i(\mathbf{q}) \neq 0$, Q is a submanifold of M . It is obvious that the above condition depends on the relative angles and, consequently, the lengths of the bars. To arrive at the condition in the statement of the theorem, we proceed from the converse.

If $g_i(\mathbf{q}) = 0$ for all i , from (3.2), we have

$$\theta_1 - \theta_0 = 0 \text{ or } \pi \tag{3.3a}$$

and

$$\theta_3 - \theta_2 = 0 \text{ or } \pi \tag{3.3b}$$

and

$$\theta_3 - \theta_0 = 0 \text{ or } \pi. \tag{3.3c}$$

Premultiplying (2.2) by $R(-\theta_0)$, we get following equivalent closure constraint equations

$$\begin{aligned}
l_0 + l_1 \cos(\theta_1 - \theta_0) + l_2 (\cos(\theta_3 - \theta_2) \cos(\theta_3 - \theta_0) + \sin(\theta_3 - \theta_2) \sin(\theta_3 - \theta_0)) \\
+ l_3 \cos(\theta_3 - \theta_2) = 0
\end{aligned} \tag{3.4a}$$

Cases	θ_{10}	θ_{32}	θ_{30}	Link Conditions	Structures
i	0	0	0	$l_0 + l_1 + l_2 + l_3 = 0$	
ii	0	0	π	$l_0 + l_1 - l_2 - l_3 = 0$	
iii	0	π	0	$l_0 + l_1 - l_2 + l_3 = 0$	
iv	0	π	π	$l_0 + l_1 + l_2 - l_3 = 0$	
v	π	0	0	$l_0 - l_1 + l_2 + l_3 = 0$	
vi	π	0	π	$l_0 - l_1 - l_2 - l_3 = 0$	
vii	π	π	0	$l_0 - l_1 - l_2 + l_3 = 0$	
viii	π	π	π	$l_0 - l_1 + l_2 - l_3 = 0$	

Table 3.1

$$\begin{aligned}
& l_1 \sin(\theta_1 - \theta_0) + l_2 (\cos(\theta_3 - \theta_2) \sin(\theta_3 - \theta_0) - \sin(\theta_3 - \theta_2) \cos(\theta_3 - \theta_0)) \\
& \quad + l_3 \sin(\theta_3 - \theta_2) = 0. \tag{3.4b}
\end{aligned}$$

So, to make θ_i 's satisfy both (3.3) and (3.4), the length of the bars should satisfy

$$l_0 + (-1)^{k_1} l_1 + (-1)^{k_2} l_2 + (-1)^{k_3} l_3 = 0 \tag{3.5}$$

for some $k_1, k_2, k_3 \in \{0, 1\}$. By contradiction, if for all $k_1, k_2, k_3 \in \{0, 1\}$ (3.5) does not hold, then there is an i such that $g_i(q) \neq 0$, which means that Q is a submanifold of M . ■

Remark 3.2: Table 3.1 summarizes the conditions on lengths of the bars which cause Q not to be a submanifold of M and the configurations with respect to the relative angles given in (3.3). It is easy to observe that case (i) can never happen since l_i are assumed to be positive. In addition, cases (iii), (iv), (v) and (vi) are trivial since, in these cases, none of the relative angles can vary, i.e. the configuration space loses one degree of freedom and the linkage becomes a rigid structure. ■

In the following we show that the condition in Theorem 3.1 can be simplified by ignoring the labels on the bars and give a topological description of Q . We first recall some definitions and results in the classical theory of mechanisms (Grashof [1883]; Paul [1979a]; Paul [1979b]).

For a four-bar linkage in classical mechanics, in which one bar, *the frame* is fixed, the following quantities are defined:

s = length of shortest bar

l = length of longest bar

p, q = lengths of intermediate bars.

A bar which is free to rotate through 2π with respect to a second bar is said to *revolve* relative to the second bar and is referred to as a *crank*. Any bar which does not revolve is called a *rocker*. If it is possible for all bars to become simultaneously aligned, such a state is called a *change point* and the linkage is said to be a *change-point mechanism*.

Theorem 3.3:(Grashof [1883])

(1) A four-bar mechanism has at least one revolving link if

$$s + l \leq p + q$$

and all three will rock if

$$s + l > p + q.$$

(2) A four-bar mechanism is a change-point mechanism iff

$$s + l = p + q.$$

■

Remark 3.4: If $s + l < p + q$, the shortest bar is the revolving bar.

It is easy to check that the cases (ii), (vii) and (viii) in Table 3.1 correspond to $s + l = p + q$, i.e. they correspond to change-point mechanisms. From Theorem 3.1, we immediately have following result.

Corollary 3.5: If $l \leq s + q + p$ and

$$s + l \neq p + q,$$

Q is a submanifold of M . ■

Remarks 3.6:

- (a) If $l > s + q + p$, the mechanism is *not constructible*.
- (b) In the sake of convenience, we refer to as the condition $s + l < p + q$ and $s + l > p + q$ as *Grashof* and *non-Grashof condition*, respectively. The corresponding linkages are referred to as *Grashof* and *non-Grashof mechanism*, respectively. We will adopt the same terminology for floating linkages also. So, Corollary 3.5 says that Q is a submanifold of M if either Grashof or non-Grashof condition holds.
- (c) It is easy to see that, given four bars, assembling them into a closed loop and labeling them sequentially, the linkage may have instantaneously one of three kinds of shape. These correspond to

$$\sin(\theta_3 - \theta_2) \begin{cases} > 0; \\ < 0; \\ = 0. \end{cases}$$

In the classical theory of mechanisms, they are called *lagging form*, *leading form* and *dead point*, respectively. ■

With above remarks in mind, we proceed to give a topological description of the configuration manifold Q . We first need the following result.

Proposition 3.7: Let $l_1 = s$. Then $s + l < p + q$ if and only if $\sin(\theta_3 - \theta_2) \neq 0$ for all configurations.

Proof: The mechanism can be assembled with s adjacent to l or with s opposite l . And, l can be l_0 , l_2 or l_3 . If $\theta_3 - \theta_2 = k\pi$, the whole structure attains a triangular shape which has the property that the sum of two sides is larger than the third one. Then it is easy to check that all possible cases will lead to

$$s + l > p + q.$$

Further, it is obvious that if $s+l = p+q$, there exist θ_2 and θ_3 such that $\sin(\theta_3 - \theta_2) = 0$. And, if $s+l > p+q$, by Grashof's theorem, all bars will rock with respect to each other. This means that dead point is reachable. Therefore, if $\sin(\theta_3 - \theta_2) \neq 0$ for all configurations, $s+l < p+q$. ■

Remark 3.8: An equivalent way to state above assertion is that a four-bar linkage is a Grashof mechanism if and only if it is constrained to be in either leading form or lagging form. Moreover, for non-Grashof mechanisms, the linkage can vary continuously from leading form to lagging form. ■

From Grashof's theorem and the above proposition we can get a topological description for Q .

Theorem 3.9:

(a) For a Grashof linkage, i.e. $s+l < p+q$, Q has two components. Each component is diffeomorphic to $R^2 \times S^1 \times S^1$.

(b) For a non-Grashof linkage, i.e. $s+l > p+q$, $Q = R^2 \times S^1 \times S^1$.

Proof: Our proof is based on explicit parameterization of the manifold Q . Recall that from (3.1) the dimension of Q is four. Again, we let $s = l_1$.

(a) If $s+l < p+q$, we consider the parameters $(x_0, y_0, \theta_0, \theta_1)$, where (x_0, y_0) is the coordinate of any point on 0-th bar in inertial frame. From the definitions of θ_0 and θ_1 and the Grashof theorem, both θ_0 and θ_1 can vary from $-\pi$ to π independently. From the remark following Proposition 3.7, one component of the manifold Q corresponds to leading form. The other corresponds to lagging form.

(b) If $s+l > p+q$, from Grashof theorem, there exists an angle α , $0 < \alpha < \pi$, such that, $\theta_{10} \in [-\alpha + \pi, \alpha + \pi]$. At the boundaries, the system is at "dead point" (see Remark 3.6 (c)). Now, we consider the independent parameters $(x_0, y_0, \theta_0, \hat{\theta})$, where

$$\hat{\theta} = \begin{cases} -\frac{\theta_{10} - \pi - \alpha}{\alpha} \frac{\pi}{2}, & \text{if } \sin(\theta_{32}) \geq 0 \text{ (lagging form);} \\ \frac{\theta_{10} - \pi - \alpha}{\alpha} \frac{\pi}{2}, & \text{if } \sin(\theta_{32}) < 0 \text{ (leading form).} \end{cases}$$

It is easy to check that $\hat{\theta}$ and θ_{10} have a one-to-one relation in both leading form and lagging form. Moreover, $\hat{\theta}$ varies from $-\pi$ to π . For $\hat{\theta} \in (-\pi, 0)$, the mechanism is in the leading form; for $\hat{\theta} \in [0, \pi]$, the mechanism is in lagging form. So $(x_0, y_0, \theta_0, \hat{\theta})$ parameterize $R^2 \times S^1 \times S^1$. ■

Remarks 3.10:

- (1) Gibson and Newstead in (Gibson & Newstead [1986]) proved above assertion through the methods of algebraic geometry.
- (2) This theorem says that for fixed point in R^2 , the configuration space is the disjoint union of two tori for a Grashof linkage and a torus for a non-Grashof linkage. For the latter, the torus can be split into two parts, one corresponding to leading form, the other corresponding to lagging form.
- (3) From the above remark, we note that, for both Grashof and non-Grashof linkages, one *may* use $(x_0, y_0, \theta_0, \theta_1)$ and specified form (leading or lagging) to parameterize Q *locally*. For non-Grashof case, one has to worry about the parameterization in the neighborhood of dead point. This problem can be solved by re-labeling the bars. We will discuss it further in the next section. ■

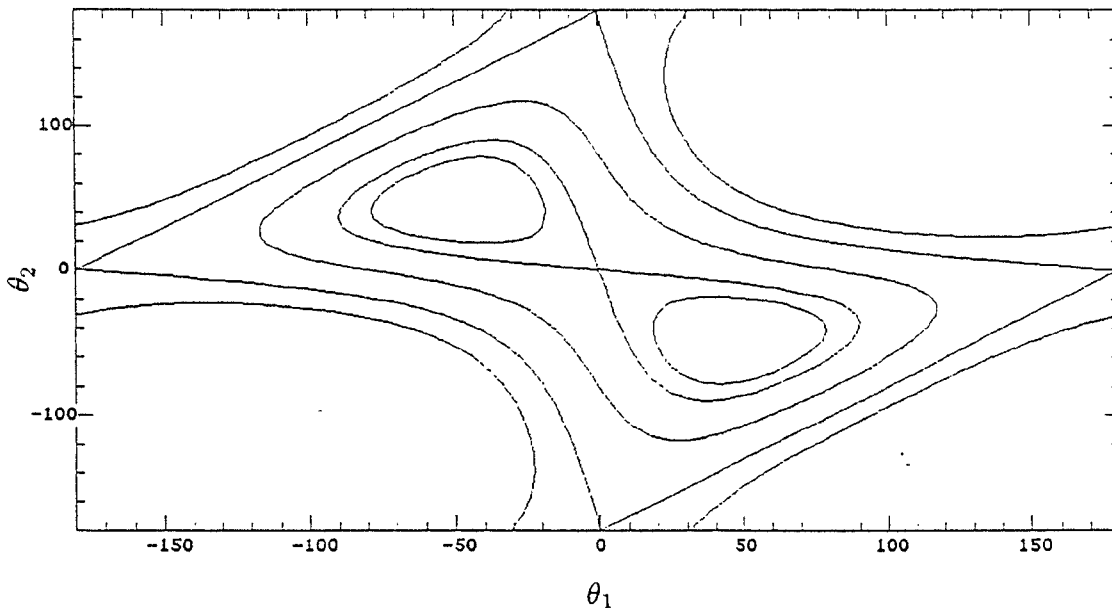


Figure 3.1 The reduced configurations, an example.

Example 3.11: Here we illustrate the Theorems 3.1 and 3.9 by a simple example. First, we fix one bar (position and orientation), say l_0 and let $\theta_0 = 0$. This means a point in $R^2 \times S^1$ has been chosen and the dimension of the configuration is reduced to one. Now the constraint equation (2.2) becomes

$$l_0 + l_1 \cos(\theta_1) + l_2 \cos(\theta_2) + l_3 \cos(\theta_3) = 0$$

$$l_1 \sin(\theta_1) + l_2 \sin(\theta_2) + l_3 \sin(\theta_3) = 0.$$

Eliminating one more angle, say θ_3 , we get

$$f(\theta_1, \theta_2) \triangleq (l_0 + l_1 \cos(\theta_1) + l_2 \cos(\theta_2))^2 + (l_1 \sin(\theta_1) + l_2 \sin(\theta_2))^2 - l_3^2 = 0. \quad (3.6)$$

The solutions of this equation gives a curve on a torus T^2 as the configuration space.

Now we choose $l_0 = 3$, $l_1 = 3$, $l_3 = 4$ and let l_2 vary. Figure 3.1 shows the results. The rectangle with opposite edges identified is the standard way to represent a torus (Guillemin & Pollack [1974]). We see that when $l_2 = 1.9$, $s + l < p + q$ holds and the solution of (3.6) on T^2 is a disconnected closed curve; when $l_2 = 2$, $s + l = p + q$ holds and the solution of (3.6) on T^2 is a “figure 8”; when $l_2 = 3$, $s + l > p + q$ holds and the solution of (3.6) on T^2 is a connected closed curve; when $l_2 = 4$, $s + l = p + q$ holds and the solution of (3.6) on T^2 is a “figure 8”, again; when $l_2 = 4.5$, $s + l > p + q$ holds and the solution of (3.6) on T^2 is a single closed curve, again. If the linkage is allowed to float, we get the configuration spaces described in Theorem 3.9. ■

4. KINETIC ENERGY

In this section we derive the kinetic energy, or lagrangian since we assumed that no potential energy is involved, for the whole system. The basic idea is to write the kinetic energy for each individual body first and then use the constraint equations to eliminate extra variables.

The kinetic energy of the i -th bar is

$$T_i = \frac{1}{2}\omega_i^2 I_i + \frac{1}{2}m_i \|\dot{\mathbf{r}}_i\|^2$$

where $\omega_i = \dot{\theta}_i$. The total kinetic energy is

$$T = \frac{1}{2} \sum_{i=0}^3 \omega_i^2 I_i + \frac{1}{2} \sum_{i=0}^3 m_i \|\dot{\mathbf{r}}_i\|^2. \quad (4.1)$$

To describe the kinetic energy relative to the center of mass, we have following useful equations,

$$\mathbf{r}_i = \mathbf{r}_c + \mathbf{r}_i^c \quad i = 0, 1, 2, 3 \quad (4.2)$$

$$\sum_{i=0}^3 m_i \mathbf{r}_i^c = 0. \quad (4.3)$$

By applying (4.2) and (4.3), (4.1) becomes,

$$T = \frac{1}{2} \sum_{i=0}^3 \omega_i^2 I_i + \frac{1}{2} \sum_{i=0}^3 m_i \|\dot{\mathbf{r}}_i^c\|^2 + \frac{1}{2} m \|\dot{\mathbf{r}}_c\|^2. \quad (4.4)$$

Applying (2.1) and (4.2), we get

$$\begin{aligned} \mathbf{r}_i^c = & \frac{1}{m} [R(\theta_{i-1})m_{i-1}\mathbf{d}_{i-1,i} \\ & - R(\theta_i)(m_{i-1}\mathbf{d}_{i,i-1} + (m_{i+1} + m_{i+2})\mathbf{d}_{i,i+1}) \\ & + R(\theta_{i+1})((m_{i+1} + m_{i+2})\mathbf{d}_{i+1,i} - m_{i+2}\mathbf{d}_{i+1,i+2}) \\ & + R(\theta_{i+2})m_{i+2}\mathbf{d}_{i+2,i+1}] \end{aligned}$$

for $i = 0, 1, 2, 3 \pmod{4}$. Note that the convention on the subscript can be used because of the closed-loop condition. Furthermore,

$$\begin{aligned} \dot{\mathbf{r}}_i^c = & \frac{1}{m} [m_{i-1}\dot{\omega}_{i-1}R(\theta_{i-1})\mathbf{d}_{i-1,i} \\ & - \dot{\omega}_i R(\theta_i)(m_{i-1}\mathbf{d}_{i,i-1} + (m_{i+1} + m_{i+2})\mathbf{d}_{i,i+1}) \\ & + \dot{\omega}_{i+1} R(\theta_{i+1})((m_{i+1} + m_{i+2})\mathbf{d}_{i+1,i} - m_{i+2}\mathbf{d}_{i+1,i+2}) \\ & + \dot{\omega}_{i+2} R(\theta_{i+2})m_{i+2}\mathbf{d}_{i+2,i+1}] \end{aligned} \quad (4.5)$$

for $i = 0, 1, 2, 3 \pmod{4}$, where

$$\tilde{\omega}_i = \begin{pmatrix} 0 & -\omega_i \\ \omega_i & 0 \end{pmatrix}.$$

By substituting the formula for $\dot{\mathbf{r}}_i^c$ into (4.4), we get a more compact expression for the kinetic energy

$$T = \frac{1}{2} \langle \tilde{\omega}, \tilde{\mathbf{J}}\tilde{\omega} \rangle + \frac{1}{2}m\|\dot{\mathbf{r}}_c\|^2 \quad (4.6)$$

where $\tilde{\omega} = (\omega_0, \omega_1, \omega_2, \omega_3)^T$ and $\tilde{\mathbf{J}} = (\tilde{J}_{i,j}, i, j = 0, 1, 2, 3)$ is a 4×4 symmetric matrix, with elements given as follows.

Let

$$\begin{aligned} M_i^I &= \frac{1}{m^2} [m_i m_{i+1} (m_i + m_{i+1}) \\ &\quad + m_{i+1} (m_{i+1} m_{i-1} + m_i m_{i+2}) \\ &\quad + m_i m_{i+2} (m_{i+1} + m_{i+2})] \end{aligned} \quad (4.7a)$$

$$M_i^{II} = \frac{m_i}{m^2} (m_{i+2}^2 - m_{i+1} m_{i-1}) \quad (4.7b)$$

$$M_i^{III} = \frac{m_i m_{i+2}}{m^2} (m_{i+1} + m_{i-1}). \quad (4.7c)$$

Then

$$\begin{aligned} \tilde{J}_{ii} &= I_i + M_i^I \|\mathbf{d}\|_{i,i+1}^2 + M_{i-1}^I \|\mathbf{d}\|_{i,i-1}^2 \\ &\quad - 2M_{i-1}^{II} \langle \mathbf{d}_{i,i+1}, \mathbf{d}_{i,i-1} \rangle \end{aligned} \quad (4.8a)$$

$$\begin{aligned} \tilde{J}_{i,i+1} &= -M_i^I \langle \mathbf{d}_{i,i+1}, R(\theta_{i+1,i})\mathbf{d}_{i+1,i} \rangle \\ &\quad + M_i^{II} \langle \mathbf{d}_{i,i+1}, R(\theta_{i+1,i})\mathbf{d}_{i+1,i+2} \rangle \\ &\quad + M_{i-1}^{II} \langle \mathbf{d}_{i,i-1}, R(\theta_{i+1,i})\mathbf{d}_{i+1,i} \rangle \\ &\quad + M_i^{III} \langle \mathbf{d}_{i,i-1}, R(\theta_{i+1,i})\mathbf{d}_{i+1,i+2} \rangle \end{aligned} \quad (4.8b)$$

$$\begin{aligned} \tilde{J}_{i,i+2} &= -M_i^{II} \langle \mathbf{d}_{i,i+1}, R(\theta_{i+2,i})\mathbf{d}_{i+2,i+1} \rangle \\ &\quad - M_{i+1}^{III} \langle \mathbf{d}_{i,i+1}, R(\theta_{i+2,i})\mathbf{d}_{i+2,i-1} \rangle \\ &\quad - M_{i+2}^{II} \langle \mathbf{d}_{i,i-1}, R(\theta_{i+2,i})\mathbf{d}_{i+2,i-1} \rangle \\ &\quad - M_i^{III} \langle \mathbf{d}_{i,i-1}, R(\theta_{i+2,i})\mathbf{d}_{i+2,i+1} \rangle \end{aligned} \quad (4.8c)$$

for $i = 0, 1, 2, 3 \pmod{4}$.

Remark 4.1: In (4.6), θ_i and the velocities ω_i , $i = 0, 1, 2, 3$ are involved. Since the whole linkage forms a closed loop, these variables are not independent. Let $l_1 = s$. By the Implicit Function Theorem one can show that given a point $(\theta_0, \theta_1, \theta_2, \theta_3)$ in $S^1 \times S^1 \times S^1 \times S^1$, such that (2.2) and $\sin(\theta_3 - \theta_2) \neq 0$ are satisfied, around this point there exists a neighborhood in which θ_2 and θ_3 can be represented as the functions of (θ_0, θ_1) uniquely. For a Grashof linkage, from Proposition 3.7, this condition is satisfied everywhere in Q . But for non-Grashof linkages this condition is satisfied *almost* everywhere in Q , except at dead points. We note however that even in this case all four bars cannot be aligned. So at such points, θ_0 and θ_1 can be represented as the functions of (θ_2, θ_3) uniquely. This is equivalent to relabeling the four bars such that $\sin(\theta_3 - \theta_2) \neq 0$. Moreover, from (Paul [1979a]), locally, there exist two functions f_1 and f_2 of $(\theta_1 - \theta_0)$ such that

$$\theta_2 = \theta_0 + f_1(\theta_1 - \theta_0)$$

$$\theta_3 = \theta_0 + f_2(\theta_1 - \theta_0).$$

We note that the expressions for functions f_1 and f_2 depend on the sign of $\sin(\theta_3 - \theta_2)$, i.e. on whether the linkage is in leading form or lagging form. Therefore, we conclude that at every point on Q , every element of the matrix $\tilde{\mathbf{J}}$ can be expressed as a function of $\theta_1 - \theta_0$. ■

Differentiating the loop constraints (2.2), one can get a relation between (ω_0, ω_1) and (ω_2, ω_3) :

$$\begin{pmatrix} \omega_2 \\ \omega_3 \end{pmatrix} = \Omega \begin{pmatrix} \omega_0 \\ \omega_1 \end{pmatrix} \quad (4.9a)$$

where

$$\Omega = \begin{pmatrix} -\frac{l_0 \sin(\theta_3 - \theta_0)}{l_2 \sin(\theta_3 - \theta_2)} & -\frac{l_1 \sin(\theta_3 - \theta_1)}{l_2 \sin(\theta_3 - \theta_2)} \\ \frac{l_0 \sin(\theta_2 - \theta_0)}{l_3 \sin(\theta_3 - \theta_2)} & \frac{l_1 \sin(\theta_2 - \theta_1)}{l_3 \sin(\theta_3 - \theta_2)} \end{pmatrix}. \quad (4.9b)$$

Again, following the same line of reasoning as in Remark 4.1, the matrix Ω is well-defined locally in general.

We summarize the above discussion in the following theorem.

Theorem 4.2: The kinetic energy of a floating four-bar linkage can be represented as

$$T = \frac{1}{2} \langle \omega, \mathbf{J}\omega \rangle + \frac{1}{2} m \|\dot{\mathbf{r}}_c\|^2 \quad (4.10)$$

where $\omega = (\omega_0, \omega_1)^T$ and

$$\mathbf{J} = (I \quad \Omega^T) \tilde{\mathbf{J}} \begin{pmatrix} I \\ \Omega \end{pmatrix}$$

for $\tilde{\mathbf{J}}$ given in (4.6)-(4.8) and Ω given in (4.9). The elements of \mathbf{J} are, locally, branched functions of $(\theta_1 - \theta_0)$ (depending $\text{sgn}(\sin(\theta_3 - \theta_2))$). ■

Before ending this section, we give a property of the matrix Ω which will be used in Sections 6 and 7.

Proposition 4.3: If Ω is well defined,

$$\begin{pmatrix} 1 \\ 1 \end{pmatrix} = \Omega \begin{pmatrix} 1 \\ 1 \end{pmatrix}.$$

Proof: Premultiplying (2.2) by $R(-\theta_2)$ and $R(-\theta_3)$, we get

$$l_0 \sin(\theta_0 - \theta_2) + l_1 \sin(\theta_1 - \theta_2) + l_3 \sin(\theta_3 - \theta_2) = 0$$

and

$$l_0 \sin(\theta_0 - \theta_3) + l_1 \sin(\theta_1 - \theta_3) + l_2 \sin(\theta_2 - \theta_3) = 0$$

respectively. The result follows immediately. ■

5. SYMMETRY, INTEGRAL AND REDUCTION

We shall show here that a floating four-bar linkage is a simple mechanical system with symmetry in the sense of Smale (Abraham & Marsden [1978]; Smale [1970]).

A *simple mechanical system with symmetry* is a 4-tuple (Q, K, V, G) , where,

- (i) (Q, K) is a Riemannian configuration manifold with metric K ;
- (ii) G is a Lie group acting on Q on the left,

$$\begin{aligned}\Phi : G \times Q &\rightarrow Q \\ (g, q) &\mapsto \Phi_g(q) \triangleq \Phi(g, q)\end{aligned}$$

such that for each $g \in G$, Φ_g is an isometry of (Q, K) ;

(iii) $V : Q \rightarrow R$ is a G -invariant potential function. The associated lagrangian is defined by

$$\begin{aligned}L : TQ &\rightarrow R \\ v_q &\mapsto L(v_q) = \frac{1}{2}K(v_q, v_q) - V \circ \tau(v_q)\end{aligned}\tag{5.1}$$

where $\tau : TQ \rightarrow Q$ is the canonical tangent projection. The Legendre transform FL of L is given here by the vector bundle isomorphism

$$K^b : TQ \rightarrow T^*Q$$

satisfying

$$K^b(v_q) \cdot w_q = K(v_q, w_q) \quad \forall v_q, w_q \in T_qQ.$$

The hamiltonian $H : T^*Q \rightarrow R$ is defined to be

$$H(\alpha_q) = \frac{1}{2}K((K^b)^{-1}(\alpha_q), (K^b)^{-1}(\alpha_q)) + V \circ \tau^*(\alpha_q)\tag{5.2}$$

where $\tau^* : T^*Q \rightarrow Q$ is the canonical cotangent projection. Letting Ω_0 denote the canonical symplectic structure (Abraham & Marsden [1978]) on T^*Q , the hamiltonian dynamics on T^*Q is given by the unique vector field X_H on T^*Q such that

$$dH(Y) = \Omega_0(X_H, Y)$$

for any vector field Y on T^*Q .

Let $\Phi^{T^*} : G \times T^*Q \rightarrow T^*Q$ be the cotangent lift of the action Φ . Denoting $\Phi_g^{T^*}(\cdot) = \Phi^{T^*}(g, \cdot)$, we have

$$H \circ \Phi_g^{T^*} = H, \quad (5.3)$$

i.e. the group G is a symmetry group of the hamiltonian system (T^*Q, Ω_0, X_H) .

The modern setting of Nother's theorem relating symmetry to the existence of integrals of motion is given by the concept of momentum mapping. Let \mathcal{G} denote the Lie algebra of G and \mathcal{G}^* its dual. The map

$$J : T^*Q \rightarrow \mathcal{G}^*$$

given by

$$J(\alpha_q) \cdot \xi = \alpha_q \cdot \xi_Q(q) \quad \forall \alpha_q \in T_q^*Q \quad (5.4)$$

is Ad^* -equivariant, where $\xi \in \mathcal{G}$ and ξ_Q is the infinitesimal generator of Φ on Q associated to ξ (see (Abraham & Marsden [1978]) corollary 4.2.11). J is a momentum mapping and the G -invariance of the hamiltonian H implies that J is an integral, i.e. it is conserved along trajectories of X_H .

Returning to four-bar linkages, we restrict attention for the moment to linkages of Grashof type, i.e. the condition $s + l < p + q$ holds. For non-Grashof case we will give a discussion in the final remark of this section. To fix the parameterization, we let $l_1 = s$. We also restrict ourselves to a connected component of the configuration space, i.e. we assume the linkage has been in either leading or lagging form. As we have seen in previous sections, the lagrangian only depends on $\theta_0 - \theta_1$ and $\dot{\theta}_0$ and $\dot{\theta}_1$. Therefore, in some essential ways, the description of the system will parallel that of a coupled two-body problem (Sreenath [1987]). In the following, we will skip some details of the proofs.

Note that the lagrangian in (4.10) does not depend on the location of the center of mass of the system. This means that the dynamics of the system is invariant under the translation in inertial space. Without loss of generality, one can place the inertial observer at the center of mass of the system. In (Sreenath et al. [1988]) this process is explained via *symplectic reduction* by the translation group R^2 . With this choice of inertial observer, the configuration space becomes

$$Q = S^1 \times S^1 \quad (5.5)$$

and the kinetic energy becomes

$$T = \frac{1}{2} \langle \omega, \mathbf{J}\omega \rangle .$$

The corresponding kinetic energy metric on Q can be defined as

$$K(w_1, w_2) = \frac{1}{2} \langle w_1, \mathbf{J}w_2 \rangle \quad (5.6)$$

for $w_1, w_2 \in T_q Q$. It is easy to observe that the group of rigid motions of this system is the symmetry group $G = S^1$. Denoting a point in Q by (θ_0, θ_1) , the action Φ of this group on Q is given by

$$\Phi(\phi, (\theta_0, \theta_1)) = (\theta_0 + \phi, \theta_1 + \phi). \quad (5.7)$$

The hamiltonian is given by

$$H = \frac{1}{2} \langle \mu, \mathbf{J}^{-1}\mu \rangle \quad (5.8)$$

for $\mu = K^b(\omega) = (\mu_0, \mu_1)$. Using the abstract formula (5.4) and the action (5.7), one can show that a momentum mapping for the action Φ is represented by

$$J(\theta, \mu) \cdot \xi = \mu_0 + \mu_1 \quad (5.9)$$

where

$$\xi = \begin{pmatrix} 0 & -1 \\ 1 & 0 \end{pmatrix} \in so(2)$$

Of course, $\nu = \mu_0 + \mu_1$ is conserved along trajectories of X_H for the hamiltonian H in (5.8) and it is simply the net angular momentum of the floating four bar linkage relative to an observer at the system center of mass.

The dynamical trajectories are confined to a level set of the form $J^{-1}(\nu)$. The group S^1 viewed as the isotropy subgroup of the momentum value ν , acts freely on $J^{-1}(\nu)$ and one gets the symplectically reduces dynamics X_{H_ν} on the reduced phase space $P_\nu = J^{-1}(\nu)/S^1 \simeq S^1 \times R^1$.

As in (Sreenath et al. [1988]) it is also possible to Poisson-reduce the dynamics. We recall that given a symplectic manifold (M, ω) , and a smooth, free, proper, symplectic action of Lie group G on M , the canonical Poisson structure on M defined by

$$\{f, g\}_M = \omega(X_f, X_g) \quad \forall f, g \in C^\infty(M)$$

descends to a Poisson structure on the quotient $P = M/G$. The latter is defined by

$$\{\hat{f}, \hat{g}\}_{M/G} \circ \pi = \{\hat{f} \circ \pi, \hat{g} \circ \pi\}_M \quad (5.10)$$

where $\hat{f}, \hat{g} \in C^\infty(M/G)$ and $\pi : M \rightarrow M/G$ is the canonical projection. If $H : M \rightarrow R$ is a G -invariant hamiltonian, it induces $\hat{H} : M/G \rightarrow R$ defined by $\hat{H} \circ \pi = H$. We refer to the dynamics (vector field) $X_{\hat{H}}$ defined by

$$X_{\hat{H}}(\hat{f}) = \{\hat{f}, \hat{H}\} \quad \forall \hat{f} \in C^\infty(M/G) \quad (5.11)$$

as the Poisson reduction of the dynamics X_H .

In the present context, with Q, K, H as in (5.5)-(5.8), the space $M = T^*(S^1 \times S^1)$ with parameterization $(\theta_0, \theta_1, \mu_0, \mu_1)$ carries the Poisson structure,

$$\{f, g\} = \sum_{i=0}^1 \left(\frac{\partial f}{\partial \theta_i} \cdot \frac{\partial g}{\partial \mu_i} - \frac{\partial f}{\partial \mu_i} \cdot \frac{\partial g}{\partial \theta_i} \right) \quad (5.12)$$

for all $f, g \in C^\infty(T^*(S^1 \times S^1))$. The action of $G = S^1$ on Q given by (5.7) is free and proper. The quotient $P = T^*(S^1 \times S^1)/S^1 \simeq S^1 \times R^2$ carries a reduced Poisson structure. Parameterizing $P = T^*(S^1 \times S^1)/S^1$ by $(\theta_{10}, \mu_0, \mu_1)$, the Poisson bracket on P is given by,

$$\{\hat{f}, \hat{g}\}_{T^*(S^1 \times S^1)/S^1} = \frac{\partial \hat{f}}{\partial \theta_{10}} \cdot \left(\frac{\partial \hat{g}}{\partial \mu_1} - \frac{\partial \hat{g}}{\partial \mu_0} \right) - \frac{\partial \hat{g}}{\partial \theta_{10}} \cdot \left(\frac{\partial \hat{f}}{\partial \mu_1} - \frac{\partial \hat{f}}{\partial \mu_0} \right) \quad (5.13)$$

which is a noncanonical structure. The reduced hamiltonian \hat{H} is given by

$$\hat{H}(\theta_{10}, \mu_0, \mu_1) = H(\theta_0, \theta_1, \mu_0, \mu_1), \quad (5.14)$$

since \mathbf{J} in (5.8) is a matrix of functions of the difference $\theta_{10} = \theta_1 - \theta_0$ only. The reduced dynamics is then immediately given:

$$\begin{aligned} \dot{\mu}_0 &= \frac{\partial \hat{H}}{\partial \theta_{10}} \\ \dot{\mu}_1 &= -\frac{\partial \hat{H}}{\partial \theta_{10}} \\ \dot{\theta}_{10} &= \frac{\partial \hat{H}}{\partial \mu_1} - \frac{\partial \hat{H}}{\partial \mu_0}. \end{aligned} \quad (5.15)$$

Equation (5.15) involves complicated analytic expressions resulting from the substitutions for θ_3 and θ_2 in terms of θ_0 and θ_1 as in (Paul [1979a]). Certain qualitative aspects of the reduced dynamics can still be explored such as relative equilibria which we will investigate in the following section.

Remark 5.1: For non-Grashof mechanisms, the system still has symmetry group $G = S^1$. This is clear if one thinks a four-bar linkage as an open four-bar chain combined with constraint equation which is invariant under the action of G . It is also clear that, in this case, if θ_0 and θ_1 are just parameters of $S^1 \times S^1$, instead of real angles of 0-th and 1-st bars, all of results in this section are valid. However, for convenience, in next two sections we will still use physical angles θ_0 and θ_1 for non-Grashof mechanisms. Then, θ_0 and θ_1 will play the role of *local coordinates* for $S^1 \times S^1$ and, consequently, (5.9), (5.13) and (5.15) will be the expressions of momentum, reduced Poisson bracket and reduced dynamics in local coordinates, respectively. ■

One of the advantages of applying reduction theory to mechanical systems is that it helps to make the dynamics of the system more transparent. For our system which is of four dimensions in phase space, the reduction process make it possible to display the dynamics by the phase portrait on a two-dimensional surface. To illustrate this, we show two examples here.

Example 5.2:

Consider a floating four-bar linkage whose parameters satisfy the Grashof condition and which is of lagging form. In particular, the parameters are chosen as the following.

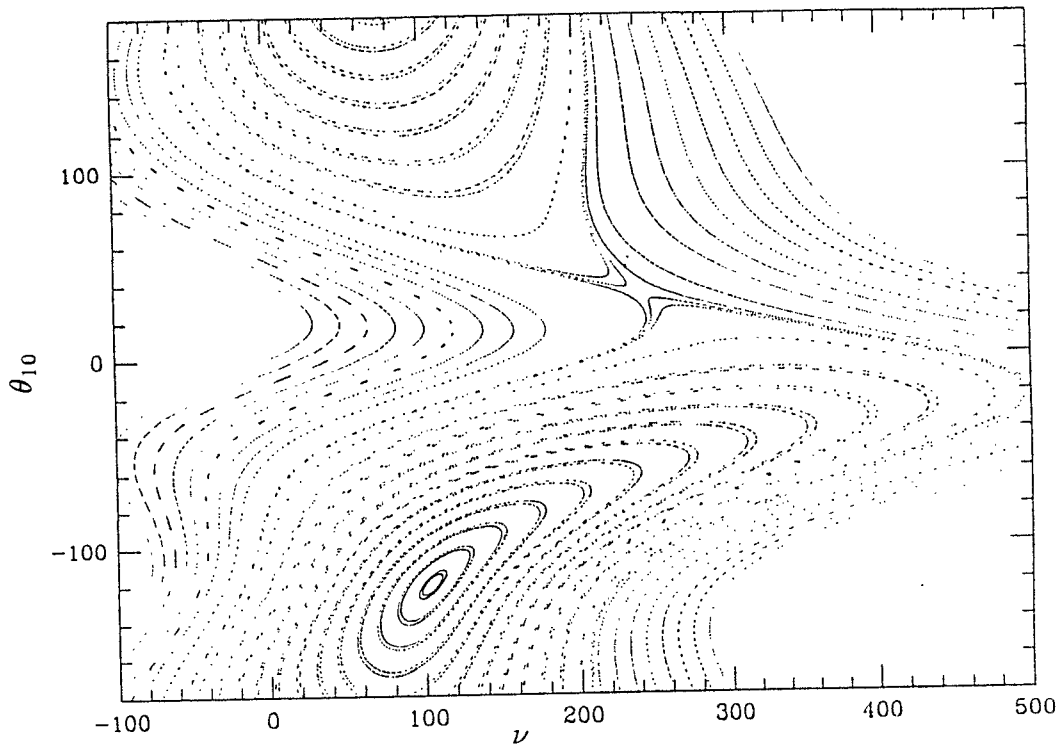
$$m_0 = 1, \quad m_1 = 1, \quad m_2 = 1, \quad m_3 = 1;$$

$$I_0 = 1, \quad I_1 = 1, \quad I_2 = 1, \quad I_3 = 1;$$

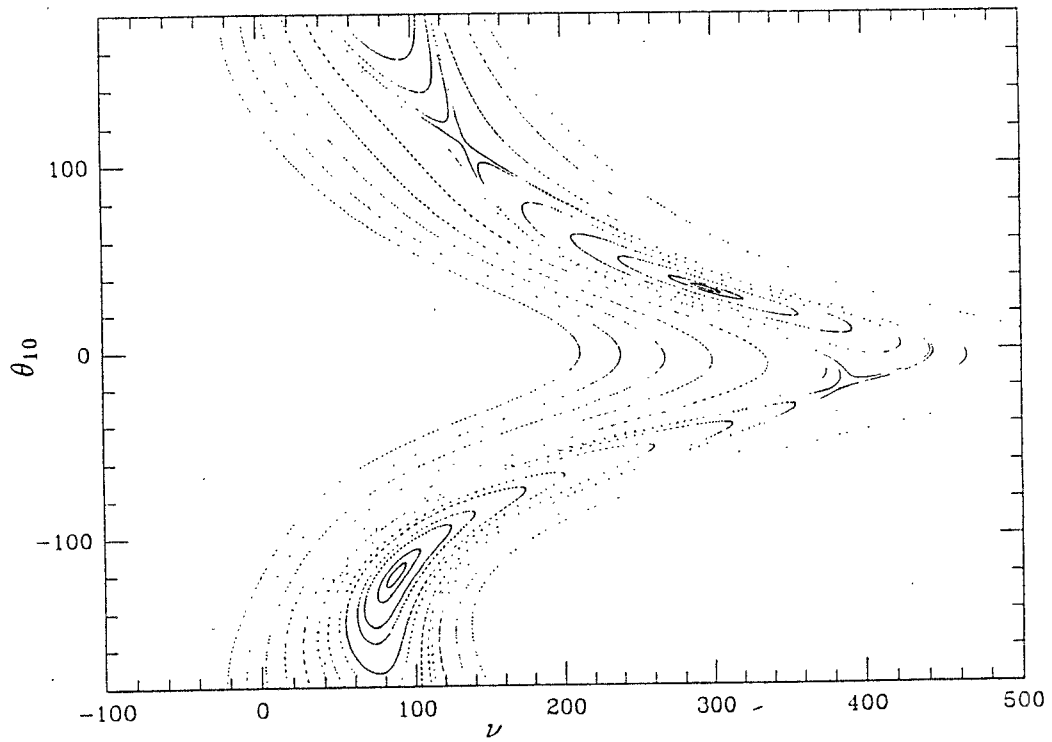
$$\mathbf{d}_{03} = (-1.5, 1), \quad \mathbf{d}_{01} = (1.5, 1), \quad \mathbf{d}_{10} = (-0.5, 1.3), \quad \mathbf{d}_{12} = (0.5, 1.3),$$

$$\mathbf{d}_{21} = (-1.5, 1), \quad \mathbf{d}_{23} = (1.5, 1), \quad \mathbf{d}_{32} = (-2, \lambda), \quad \mathbf{d}_{30} = (2, \lambda).$$

Following the same procedure as in (Sreenath et al. [1988]), the dynamics can be further reduced to a symplectic leaf. The hamiltonian on a leaf is a function of θ_{10} and



(a) $\lambda = 0$



(b) $\lambda = -5$

Figure 5.1 The phase portraits for a Grashof linkage

$\nu (= \frac{1}{2}(\mu_1 - \mu_0))$ and the dynamics on the leaf is given by

$$\frac{d\theta_{10}}{dt} = \frac{\partial H}{\partial \nu}(\theta_{10}, \nu), \quad \frac{d\nu}{dt} = -\frac{\partial H}{\partial \theta_{10}}(\theta_{10}, \nu)$$

Therefore, for fixed value of angular momentum, one can draw the phase portrait on a cylinder with θ_{10} versus ν . Figure 5.1 shows the phase portraits for $\lambda = 0$ and $\lambda = -5$, respectively. On Figure 5.1(a), we see there is one center and one saddle point. However, in Figure 5.1(b), there are two centers and two saddles. The difference is caused by an offset in the position of center of mass of 3rd bar from the line connecting the two joints on that bar. ■

Example 5.3:

Consider a floating four-bar linkage whose parameters satisfy the non-Grashof condition and the parameters are chosen as the following.

$$m_0 = 1, \quad m_1 = 1, \quad m_2 = 1, \quad m_3 = 1;$$

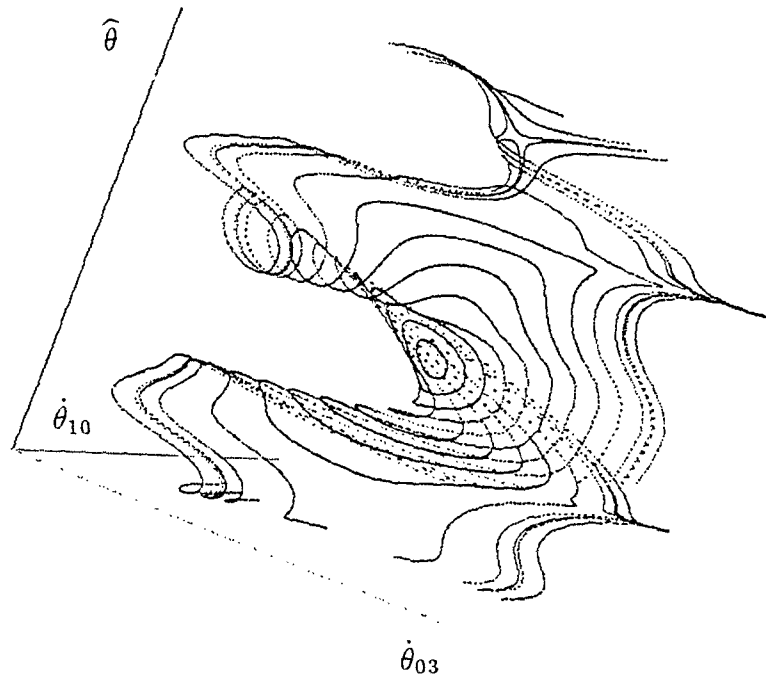
$$I_0 = 1, \quad I_1 = 1, \quad I_2 = 1, \quad I_3 = 1;$$

$$\mathbf{d}_{03} = (-2, \lambda), \quad \mathbf{d}_{01} = (2, \lambda), \quad \mathbf{d}_{10} = (-1.5, -1), \quad \mathbf{d}_{12} = (1.5, -1),$$

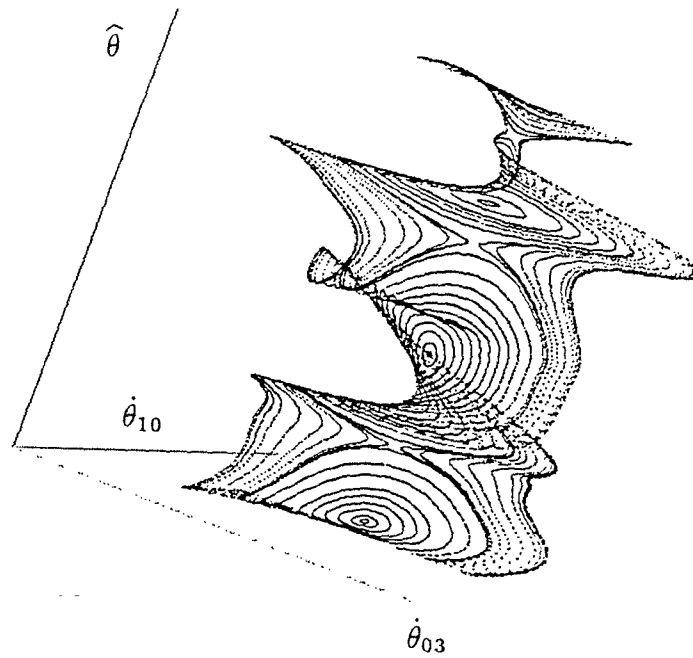
$$\mathbf{d}_{21} = (-1.5, -1.4), \quad \mathbf{d}_{23} = (1.5, -1.4), \quad \mathbf{d}_{32} = (-1.5, -1), \quad \mathbf{d}_{30} = (1.5, -1).$$

Instead of displaying the dynamics on position-momentum phase space, here we try to show it on position-velocity phase space. Since the dynamics cannot be further reduced so that it depends on one relative angle and corresponding angular velocity, one has to display the phase portrait in three dimensional space. For a given angular momentum, the phase portrait sits on a surface in this space. In this example, this space is parameterized by $(\dot{\theta}_{10}, \hat{\theta}, \dot{\theta}_{03})$. Figure 5.2 shows the phase portraits corresponding to $\lambda = -15$ and $\lambda = 0$, respectively. From Figure 5.2, we see, again, the change of numbers of centers and saddles. ■

In the next section, we will show how to compute the centers and saddle points and associated bifurcations.



(a) $\lambda = -15$



(b) $\lambda = 0$

Figure 5.2 The phase portraits for a non-Grashof linkage

6. RELATIVE EQUILIBRIA AND BIFURCATIONS

We first give the definition of relative equilibria and recall Smale's theorem (Smale [1970]).

For a hamiltonian system (M, ω, X_H) where M is a $2n$ -dimensional smooth manifold, ω is a symplectic form on M , X_H is hamiltonian vector field determined by

$$i_{X_H}\omega = dH$$

for some smooth hamiltonian function H on M . For simple mechanical systems, $M = T^*Q$, the cotangent bundle of the configuration space Q , of the system. Let G be a symmetry group acting on Q on the left,

$$\begin{aligned} \Phi : G \times Q &\rightarrow Q \\ (g, q) &\mapsto \Phi_g(q) \triangleq \Phi(g, q), \end{aligned}$$

and hence on T^*Q by cotangent lift. The following definition of a relative equilibrium is standard (Abraham & Marsden [1978]).

Definition 6.1: Let $F_{X_H}^t$ be the flow of X_H on M . Then $z_e \in M$ is a relative equilibrium if $F_{X_H}^t(z_e)$ is a stationary motion, i.e. there exists $\xi \in \mathcal{G}$ such that

$$F_{X_H}^t(z_e) = \exp(t\xi)(z_e),$$

where \mathcal{G} is the Lie algebra of the group G . ■

Remarks 6.2:

- (1) Let $X_{\hat{H}}$ be the Poisson reduced vector field as shown in (5.11). Then z_e is a relative equilibrium iff

$$X_{\hat{H}}(\pi(z_e)) = 0.$$

- (2) A physical interpretation of relative equilibria is that if the dynamics of a system is rotationally invariant, the dynamical orbit of a relative equilibrium appears to be a fixed point for an observer in a suitable uniformly rotating coordinate system. ■

Given a simple mechanical system with symmetry, (Q, K, V, G) , which is defined in section 5, we have following theorem by Smale.

Hence, by Theorem 6.3, (θ_e, μ_e) is a relative equilibrium point on T^*Q iff θ_e is a critical point of the function

$$V_\xi(\theta_0, \theta_1) = -\xi^2(1, 1)\mathbf{J} \begin{pmatrix} 1 \\ 1 \end{pmatrix}$$

where $\theta_e = ((\theta_0)_e, (\theta_1)_e)$ and $\mu_e = ((\mu_0)_e, (\mu_1)_e)$. Applying Proposition 4.3 and the 4×4 matrix $\tilde{\mathbf{J}}$ defined in Theorem 4.2, we have

$$V_\xi(\theta_0, \theta_1) = -\xi^2 \mathbf{e}^T \tilde{\mathbf{J}} \mathbf{e} \quad (6.5)$$

where $\mathbf{e} = (1 \ 1 \ 1 \ 1)^T$. Since the elements of matrix $\tilde{\mathbf{J}}$ are, locally, functions of $\theta_1 - \theta_0$ or constants, the above V_ξ satisfies (6.2) for all $g \in S^1$. It follows that

$$\hat{V}_\xi(\theta_{10}) = V_\xi(\theta_0, \theta_1).$$

Then, the critical points θ_e of V_ξ will make $((\theta_1)_e - (\theta_0)_e)$ to be the critical points of \hat{V}_ξ . At relative equilibrium, the relative angles between bars keep unchanged and the whole system rotates around the system center of mass with constant angular velocity.

Remarks 6.5:

- (1) It should be noted that, in general, given the value of $((\theta_1)_e - (\theta_0)_e)$ one cannot tell what the relative equilibrium shape of the linkage looks like. The particular form (leading or lagging) has to be indicated at the same time.
- (2) \hat{V}_ξ with $\xi = 1$ is the *locked inertia*. Its value at θ_{10} equals to the value of the moment of inertia of the corresponding frozen system, i.e. the system with all joints locked, about its center of mass. The above result shows that a relative equilibrium shape corresponds to a frozen system which has maximum or minimum value of moment of inertia within all possible frozen systems. Since at relative equilibrium ξ is a constant, we will let $\xi = 1$ later. ■

In the rest of this section, we are particularly interested in assemblies which admit configurations with reflection symmetry, which will be called *symmetric configuration*. Applying the notations in Section 2, a floating four-bar linkage is of *symmetric type* if, with proper consecutive labeling of the bars,

$$m_1 = m_3, \quad l_1 = l_3 \quad (6.6a)$$

$$|\mathbf{d}_{01}| = |\mathbf{d}_{03}|, |\mathbf{d}_{10}| = |\mathbf{d}_{30}|, |\mathbf{d}_{12}| = |\mathbf{d}_{32}|, |\mathbf{d}_{21}| = |\mathbf{d}_{23}| \quad (6.6b)$$

and

$$\mathbf{d}_{10}^T \begin{pmatrix} 0 & 0 \\ 0 & 1 \end{pmatrix} \mathbf{d}_{30} > 0. \quad (6.6c)$$

In other words it can form symmetric shapes as shown in Figure 6.1. It is not hard to verify that any four-bar linkage which satisfies (6.6) has two such symmetric configurations.

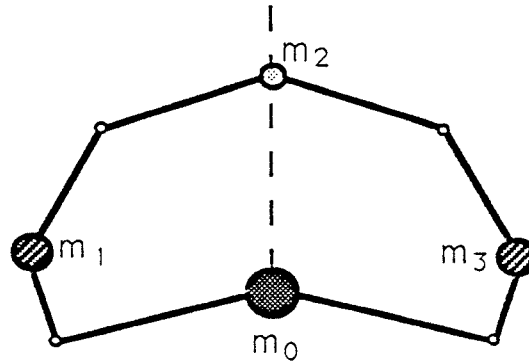


Figure 6.1 A Symmetric Configuration

Although it is not easy to find the critical points of \hat{V}_ξ analytically, for a particular example one can easily find them numerically. Unlike the planar two body problem (Sreenath [1987]) for which the dimension of the shape space is also one, here the function \hat{V}_ξ has many parameters. A natural question is to determine how these parameters affect the relative equilibria, e.g. their numbers and location on shape space, etc.. *Of course, it is difficult to answer this question for completely arbitrary choice of parameters.* However, by leaving one particular parameter free such that the assembly preserves its symmetric configurations and freezing all other parameters, one still can observe a nontrivial bifurcation phenomenon. To illustrate this we consider an example.

Example 6.6: Let us choose the parameters as follows.

$$m_0 = 1, \quad m_1 = 1, \quad m_2 = 1, \quad m_3 = 1;$$

$$\mathbf{d}_{03} = (-2, \lambda_0), \quad \mathbf{d}_{01} = (2, \lambda_0), \quad \mathbf{d}_{10} = (-1.5, -1), \quad \mathbf{d}_{12} = (1.5, -1),$$

$$\mathbf{d}_{21} = (-1.5, -1.4), \quad \mathbf{d}_{23} = (1.5, -1.4), \quad \mathbf{d}_{32} = (-1.5, -1), \quad \mathbf{d}_{30} = (1.5, -1).$$

Now the assembly has *non-Grashof* structure.

Using \hat{V}_ξ , for any λ_0 one can find relative equilibria $(\theta_{10})_e$ for both leading form and lagging form, and hence, corresponding $\hat{\theta}$ which is defined in the proof the Theorem 3.9. As λ_0 varies from $-\infty$ to $+\infty$, one can plot a diagram for $\hat{\theta}$ versus λ_0 . Figure 6.2 shows the result, in which solid dots represent stable relative equilibria, small circles represent unstable relative equilibria. ■

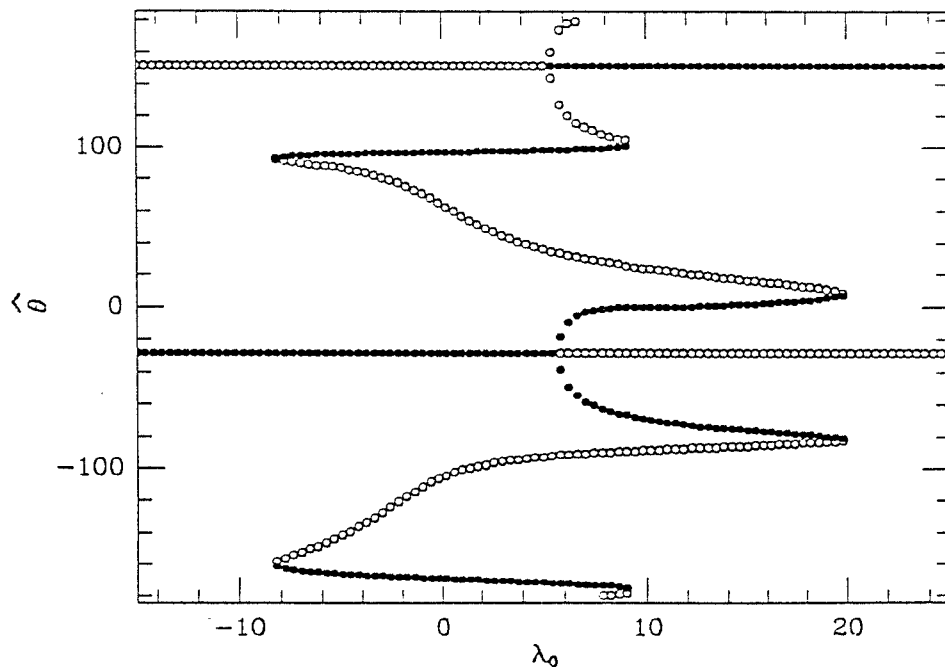


Figure 6.2 Bifurcation diagram: an example

From this example one can make the following empirical observations:

(1) There are two unbounded symmetric branches on the diagram and these branches are bifurcated at some points. The bifurcations appear to be pitchfork bifurcations.

(2) Almost any value of $\hat{\theta}$ can be a relative equilibrium for a particular λ_0 . In other words the bifurcation diagram is connected globally.

(3) The number of relative equilibria can be two, six and ten.

The first observation, which relates to the local bifurcation problem, is what we will concentrate on in the rest of this section. The others will be discussed later.

As we have seen, the function \hat{V}_ξ of a four-bar linkage is a multiple parameter function. One might expect very complicated bifurcation features with respect to these parameters. Here, instead of considering a general structure, we study a special assembly which has symmetric configuration. To avoid too many tedious calculations we particularly choose the parameters of the assembly as follows.

$$m_0 = m_1 = m_2 = m_3 = 1;$$

$$\mathbf{d}_{03} = (-d_0, \lambda_0), \quad \mathbf{d}_{01} = (d_0, \lambda_0), \quad \mathbf{d}_{10} = (-1, 0), \quad \mathbf{d}_{12} = (1, 0) \quad (6.7)$$

$$\mathbf{d}_{21} = (-d_2, \lambda_2), \quad \mathbf{d}_{23} = (d_2, \lambda_2), \quad \mathbf{d}_{32} = (-1, 0), \quad \mathbf{d}_{30} = (1, 0).$$

where d_0 and d_2 are fixed and $d_0 > d_2 > 0$, $\lambda_0, \lambda_2 \in R$. Moreover, we consider the non-Grashof case only, i.e.

$$s + l > p + q. \quad (6.8)$$

Figure 6.3 shows two symmetric configurations for the above choice of parameters. We will see that although only two parameters λ_0 and λ_2 are left to be free, the bifurcation features with respect to these parameters are still informative.

The function \hat{V}_ξ now has the following form:

$$\begin{aligned} \hat{V}_\xi = & \frac{1}{4}(2\lambda_2 \sin(\theta_{32}) + d_2 \cos(\theta_{32}) - \cos(\theta_{31}) + d_0 \cos(\theta_{30}) \\ & + 2\lambda_2 \sin(\theta_{21}) + d_2 \cos(\theta_{21}) - d_0 d_2 \cos(\theta_{20}) + d_0 \cos(\theta_{10})) \end{aligned}$$

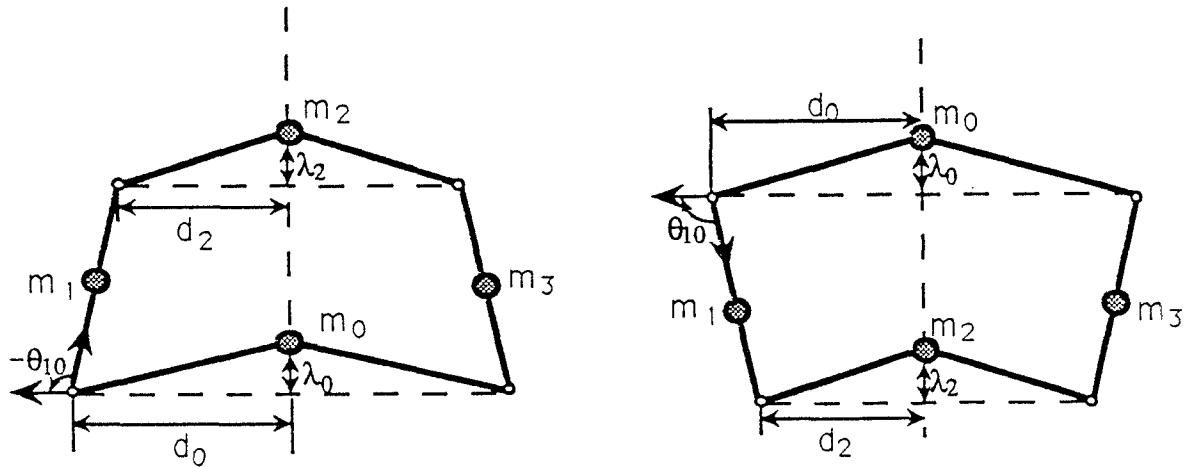


Figure 6.3 Symmetric Configurations

$$+\frac{\lambda_0}{4}(2\sin(\theta_{30}) + \lambda_2\cos(\theta_{20}) - 2\sin(\theta_{10})) + C \quad (6.9)$$

where C is a constant determined by d_{ij} , m_i and the moments of inertia of the bodies, I_i . For $i, j = 0, 1, 2, 3$, $\theta_{ij} = \theta_i - \theta_j$ and θ_i satisfy the constraint equations

$$d_0 + \cos(\theta_{10}) + d_2\cos(\theta_{20}) + \cos(\theta_{30}) = 0 \quad (6.10a)$$

$$\sin(\theta_{10}) + d_2\sin(\theta_{20}) + \sin(\theta_{30}) = 0. \quad (6.10b)$$

In the following, at symmetric configuration, the variables will be denoted by superscript “s” (say, θ_{10}^s), the formulas will be denoted by “|_s” (say, $f(\theta_{10})|_s$). As shown in the example, the bifurcation diagram of relative equilibria will be parameterized by $(\hat{\theta}, \lambda_0)$.

Theorem 6.7: For a floating four-bar linkage with parameters shown in (6.7), the bifurcation diagram of relative equilibria has the following properties:

(1) There are two infinite branches in the diagram, one corresponds to θ_{10}^s in the leading form, another one corresponds to θ_{10}^s in the lagging form. We refer to these as the symmetric branches.

(2) There exists a constant λ_2^* such that no bifurcation occurs on the symmetric branch of leading form if $\lambda_2 = \lambda_2^*$; and, no bifurcation occurs on the symmetric branch of lagging form if $\lambda_2 = -\lambda_2^*$.

(3) On the symmetric branch of leading (lagging) form, if $\lambda_2 < \lambda_2^*$ ($-\lambda_2^*$), there exists a constant c_1 (c_3) such that the relative equilibria are stable for $\lambda_0 < c_1$ (c_3), unstable for $\lambda_0 > c_1$ (c_3), bifurcated for $\lambda_0 = c_1$ (c_3); on the other hand, if $\lambda_2 > \lambda_2^*$ ($-\lambda_2^*$), there exists a constant c_2 (c_4) such that the relative equilibria are unstable for $\lambda_0 < c_2$ (c_4), stable for $\lambda_0 > c_2$ (c_4), bifurcated for $\lambda_0 = c_2$ (c_4).

(4) Assume $\lambda_2 \neq \pm\lambda_2^*$. Let

$$\epsilon^\pm = \text{sgn} \frac{\pm\epsilon_1 \lambda_2^2 + \epsilon_2 \lambda_2 \pm \epsilon_3}{\epsilon_4 \lambda_2 \pm \epsilon_5} \quad (6.11)$$

and

$$\delta^\pm = \text{sgn}(\delta_1 \lambda_2 \pm \delta_2) \quad (6.12)$$

where ϵ_i and δ_i are constants which are determined by d_0 and d_2 . Then, the bifurcation on the symmetric branch of leading form will be supercritical pitchfork if $\epsilon^+ \delta^+ < 0$. It will be subcritical pitchfork if $\epsilon^+ \delta^+ > 0$. Similarly, the bifurcation on the symmetric branch of lagging form will be supercritical pitchfork if $\epsilon^- \delta^- < 0$. It will be subcritical pitchfork if $\epsilon^- \delta^- > 0$.

Remarks 6.8:

(a) Based on the techniques of bifurcation theory shown in appendix A, the proof of the above assertions is very elementary. However, two aspects have to be considered before the bifurcation theory is applied. First, one has to determine the *existence* of a bifurcation and where the branches are bifurcated. Second, as one can see, it is not easy to write down explicitly the function \hat{V}_ξ as a function of one variable. Therefore, when applying the techniques of bifurcation theory which involves as high as fourth order derivatives of the function \hat{V}_ξ , one should consider the closure constraint equation (2.2) simultaneously.

(b) Although the proof of the above assertions is elementary, it requires a large effort in calculations. We used MACSYMA to handle these computations. In the following, we only give a sketch of the proof. ■

Proof of Theorem 6.7: Note that the function \hat{V}_ξ can be written as a function of relative angles θ_{10} , θ_{20} , and θ_{30} , which are related through constraint equations (6.10). From (6.10), we can consider (locally) θ_{20} and θ_{30} as the functions of θ_{10} . Again, from (6.10) one can generate the quantities $\frac{\partial^i \theta_{20}}{\partial \theta_{10}^i} |_s$ and $\frac{\partial^i \theta_{30}}{\partial \theta_{10}^i} |_s$ for any positive integer i . Moreover, from Figure 6.3 it is easy to see that at symmetric configuration

$$\theta_{20}^s = \pi \quad \text{and} \quad \theta_{10}^s = -\theta_{30}^s. \quad (6.13)$$

With above considerations, one can have closed form expressions for $\frac{\partial^i \theta_{20}}{\partial \theta_{10}^i} |_s$ and $\frac{\partial^i \theta_{30}}{\partial \theta_{10}^i} |_s$.

For instance,

$$\begin{cases} \frac{\partial \theta_{20}}{\partial \theta_{10}} |_s = \frac{2}{d_2} \cos(\theta_{10}^s), \\ \frac{\partial \theta_{30}}{\partial \theta_{10}} |_s = 1 \end{cases} \quad (6.14)$$

and

$$\begin{cases} \frac{\partial^2 \theta_{20}}{\partial \theta_{10}^2} |_s = \frac{2 \cos^2(\theta_{10}^s)}{d_2^2 \sin(\theta_{10}^s)} (d_2 - 2 \cos(\theta_{10}^s)), \\ \frac{\partial^2 \theta_{30}}{\partial \theta_{10}^2} |_s = \frac{2 \cos(\theta_{10}^s)}{d_2 \sin(\theta_{10}^s)} (d_2 - 2 \cos(\theta_{10}^s)) \end{cases} \quad (6.15)$$

and so on.

To prove assertion (1) in the statement of the theorem, one needs to show that at symmetric configuration, the equation

$$\frac{\partial \hat{V}_\xi}{\partial \theta_{10}} |_s = 0$$

does not depend on λ_0 . Concentrating on the term involving λ_0 in \hat{V}_ξ and applying (6.13) and (6.14), one can show that the first derivative of that term with respect to θ_{10} at symmetric configuration is zero. Since the rest of the terms of $\frac{\partial \hat{V}_\xi}{\partial \theta_{10}} |_s = 0$ are still functions of θ_{10}^s , one can see two infinite symmetric branches in the bifurcation diagram for two different θ_{10}^s . Assertion (1) is thus proved.

Applying (6.14) and (6.15), one can show that the second derivative of the function \hat{V}_ξ at symmetric configuration has the form

$$\frac{\partial^2 \hat{V}_\xi}{\partial \theta_{10}^2} |_s = \frac{\partial^2 \Pi}{\partial \theta_{10}^2} |_s - \lambda_0 \left(\frac{d_2 - 2 \cos^3(\theta_{10}^s)}{d_2 \sin(\theta_{10}^s)} + \lambda_2 \frac{\cos^2(\theta_{10}^s)}{d_2^2} \right), \quad (6.16)$$

where Π is the summation of the terms not involving λ_0 in \hat{V}_ξ . It is obvious that when

$$\lambda_2 = \lambda_2^* \triangleq \frac{2d_2 \cos^2(\theta_{10}^s) - d_2^2}{\cos^2(\theta_{10}^s) \sin(\theta_{10}^s)}, \quad (6.17)$$

$\frac{\partial^2 \hat{V}_\xi}{\partial \theta_{10}^2} \Big|_s$ will not depend on λ_0 . One can also show that with (6.17), $\frac{\partial^2 \hat{V}_\xi}{\partial \theta_{10}^2} \Big|_s \neq 0$ under assumptions (6.7) and (6.8). This means that bifurcation may not occur on either symmetric branch of leading form or symmetric branch of lagging form. Note that on these different forms $\cos(\theta_{10}^s)$ has the same value, $\sin(\theta_{10}^s)$ has the same absolute value but different sign. (See Figure 6.3) Thus, assertion (2) is proved.

As we have known earlier, the stability of relative equilibria depends on the sign of $\frac{\partial^2 \hat{V}_\xi}{\partial \theta_{10}^2} \Big|_s$. From (6.16) we see that $\frac{\partial^2 \hat{V}_\xi}{\partial \theta_{10}^2} \Big|_s$ is a linear function of λ_0 . Using the λ_2^* in (6.17), the proof of (3) is straight forward.

To prove assertion (4), we apply the bifurcation theory mentioned in appendix A. Let λ_0^* denote c_i in assertion (3) for some suitable i . One can show that at $(\theta_{10}, \lambda_0^*)$,

$$\frac{\partial \hat{V}_\xi}{\partial \theta_{10}} = \frac{\partial^2 \hat{V}_\xi}{\partial \theta_{10}^2} = \frac{\partial^3 \hat{V}_\xi}{\partial \theta_{10}^3} = \frac{\partial^2 \hat{V}_\xi}{\partial \theta_{10} \partial \lambda} = 0 \quad (6.18)$$

Moreover

$$\frac{\partial^4 \hat{V}_\xi}{\partial \theta_{10}^4}(\theta_{10}^s, \lambda_0^*) = \frac{\pm \epsilon_1 \lambda_2^2 + \epsilon_2 \lambda_2 \pm \epsilon_3}{\epsilon_4 \lambda_2 \pm \epsilon_5} \quad (6.19)$$

and

$$\frac{\partial^3 \hat{V}_\xi}{\partial \theta_{10}^2 \partial \lambda_0}(\theta_{10}^s, \lambda_0^*) = \delta_1 \lambda_2 \pm \delta_2 \quad (6.20)$$

for some constants ϵ_i and δ_i , where “+” corresponds to leading form, “-” corresponds to lagging form. See Appendix B for expressions of ϵ_i and δ_i . Since (6.19) and (6.20) are not zero in general, applying the lemma in appendix A, we can say $\frac{\partial \hat{V}_\xi}{\partial \theta_{10}}$ is strongly equivalent to the normal form of pitchfork bifurcation. In addition, the type of pitchfork bifurcation depends on the sign of (6.19) and (6.20). The assertion (4) is proved. ■

Remarks 6.9: (i) The condition of $\lambda_2 \neq \lambda_2^*$ guarantees that (6.20) and the denominator of (6.19) are not zero. (ii) In general the bifurcation changes from a supercritical one to subcritical one at the roots of numerator of (6.19). ■

Example 6.10: To see how λ_2 changes the bifurcation diagram with parameter λ_0 we give following example. We will concentrate on the symmetric branch with respect to

leading form. Let $d_0 = 2$ and $d_2 = 1$. Then ϵ and δ have the following form

$$\epsilon^+ = \operatorname{sgn} \frac{\lambda_2^2 + 6.938\lambda_2 - 3.623}{1.873 - 0.051\lambda_2}$$

$$\delta^+ = \operatorname{sgn}(1.025 - 0.028\lambda_2)$$

Then

$$\epsilon^+ \delta^+ = \begin{cases} -1, & \text{if } -7.426 < \lambda_2 < 0.488; \\ +1, & \text{otherwise.} \end{cases}$$

Note that the region for λ_2 is an approximation. So we can say that, when $\lambda_2 \in (-7.426, 0.488)$, the pitchfork bifurcation is supercritical. Otherwise, it is subcritical. Figure 6.4 shows this result. ■

Before closing this section, we would like to make a few additional remarks.

(i) Although our discussion only concentrated on a structure of non-Grashof type, a version of Theorem 6.7 also holds for the Grashof case.

(ii) Up to now we have understood the phenomenon of bifurcation on the symmetric branches. The global analysis of the bifurcations involves massive symbolic computations. However, as shown in the Example 6.6 in this section and other simulations, one can numerically determine a global bifurcation diagram. A large body of such numerical simulations show that the branches in the bifurcation diagram are connected. In other words, for any point in shape space, there is a finite λ_0 for which that shape determines a relative equilibrium. This is consistent with the linearity of \hat{V}_ξ in λ_0 . This property provides a possibility to control the attitude of a space structure with a closed kinematic chain by simply changing the position of the centers of mass of some bars.

(iii) Our results in this paper rely on some ideal conditions, for instance, the symmetry condition (6.6), and the absence of external and internal disturbances. One may ask what will happen when these conditions are violated. The answer to this question may relate to the notion of *universal unfolding* in bifurcation theory. Numerical results show that it is possible to use the unfolding property to control the shape of the structure near the bifurcation point.

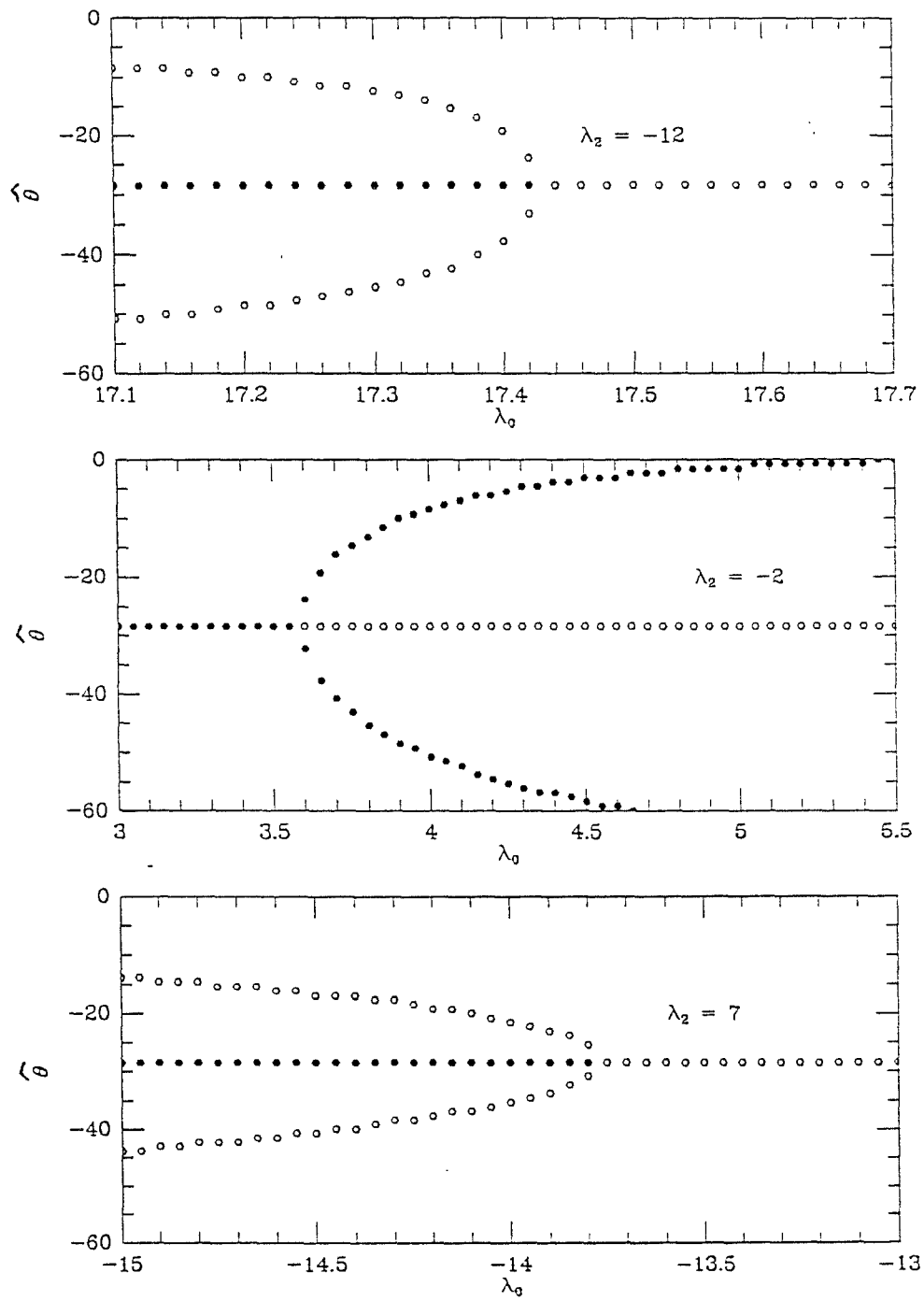


Figure 6.4 Bifurcation Diagrams

7. GEOMETRIC PHASES

Recently, it has become clear that in a variety of mechanical contexts, certain (angular) drift phenomena arise which can be understood via geometric methods. As illustrations, we note the drift in the orientation of a satellite caused by oscillations in flexible components of the satellite, the slow change in the plane of oscillation of a Foucault pendulum during a 24-hour period, the ability of trampoline artists to reorient themselves in mid-air through limb and trunk movements etc.. In the computation of such drifts, one notes that some or all of the drift may be attributable to geometric quantities such as a path integral in a space of equivalence classes (i.e. shape space) of configurations. Hence the term geometric phase is used in connection with such drifts. We refer the reader to (Shapere & Wilczek [1989]) and (Marsden, Montgomery & Ratiu [1990]) for some of the basic references and the general theory. Of direct relevance to the present paper are the computation of geometric phases in multibody systems in (Krishnaprasad [1990]; Krishnaprasad & Yang [1991]; Krishnaprasad, Yang & Dayawansa, [1991]). See also (Shapere [1989]) for an example of translational drift arising in swimming organisms. In the present section, we will compute geometric phases for the four-bar linkage and show special features arising from the presence of an closed kinematic chain. We begin with a brief summary of the abstract framework. Consider

- (a) a simple mechanical system with symmetry (Q, K, V, G) ;
- (b) a principal G -bundle $(Q, Q/G, G)$;
- (c) controls (forces) acting on (Q, K, V, G) , also leaving invariant the conserved momentum map $J^\# : TQ \rightarrow \mathcal{G}^*$ associated to the free hamiltonian system with energy $K + V$, where \mathcal{G}^* is the dual of the Lie algebra \mathcal{G} of G . The map $J^\#$ is given explicitly by the formula

$$J^\#(w_q)\xi = (K^b w_q)(\xi_Q(q))$$

where $\xi \in \mathcal{G}$, K^b is the Legendre transform and ξ_Q is the infinitesimal generator (vector field on Q) associated to ξ .

Define \mathbf{I}_q the symmetric bilinear form on \mathcal{G} by

$$\mathbf{I}_q(\xi, \eta) = K(\xi_Q(q), \eta_Q(q)).$$

Let $\mathbf{I}_q^b : \mathcal{G} \rightarrow \mathcal{G}^*$ be the corresponding pairing. Then we have a vertical-horizontal splitting of the tangent bundle TQ ,

$$\begin{aligned} TQ_q &= (Vert)_q \oplus (Hor)_q \\ w_q &= ((\mathbf{I}_q^b)^{-1}\mu)_Q(q) + (w_q - ((\mathbf{I}_q^b)^{-1}\mu)_Q(q)) \end{aligned}$$

where $\mu = J^\#(w_q)$. This splitting has the equivariance property with respect to the G -action on Q and defines a principal connection. This connection, referred to as *mechanical connection*, appears to be originally due to Smale and Kummer (see (Marsden, Montgomery & Ratiu [1990])).

In the concrete setting of *planar* many-body problems with rigid and flexible components, in which $G = S^1$ is abelian, the phase shift (angle) associated to a specific path γ in shape space $S = Q/G$ is simply the integral of the connection form over the path. For loop γ it is the *holonomy*. In (Krishnaprasad [1990]), a formula for the phase shift for a system of N planar rigid laminae connected by $(N - 1)$ single degree of freedom $(N - 1)$ pin joints is derived. For this system, the configuration space is \mathbf{T}^N parametrized by $\theta = (\theta_1, \dots, \theta_N)$ and the shape space is \mathbf{T}^{N-1} parameterized by $\phi = (\phi_1, \dots, \phi_{N-1})$, where $\phi_i = \theta_{i+1} - \theta_i$. Let

$$\gamma = \{(\phi_1(t), \dots, \phi_{N-1}(t)) | t \in [0, T], \text{ for some } T > 0\}$$

be a closed curve in \mathbf{T}^{N-1} , i.e. $\phi_i(0) = \phi_i(T)$. Then absolute reorientation or phase shift of the first body is given by

$$\Delta\theta_1 = \theta(T) - \theta(0) = \int_0^T \frac{\mu}{\mathbf{e} \cdot \mathbf{J}\mathbf{e}} dt - \int_\gamma \frac{\mathbf{e} \cdot \mathbf{J}M d\phi}{\mathbf{e} \cdot \mathbf{J}\mathbf{e}} \quad (7.1)$$

where $\mathbf{e} = (1, \dots, 1)^T \in R^N$; $M \in R^{N \times (N-1)}$ is defined by

$$M_{ij} = \begin{cases} 1 & \text{if } i > j \geq 1, \\ 0 & \text{otherwise.} \end{cases}$$

\mathbf{J} is a configuration-dependent $N \times N$ matrix, which defines a riemannian metric on \mathbf{T}^N , is invariant under the S^1 action: $(\theta_1, \dots, \theta_N) \rightarrow (\theta_1 + \theta, \dots, \theta_N + \theta)$ for $\theta \in S^1$ (in other words, it is a matrix of functions of ϕ); and, the constant $\mu = \mathbf{e} \cdot \mathbf{J}\dot{\theta}$ is angular momentum

of the system. Since γ is closed, $\Delta\theta_i = \Delta\theta_1$, for $i = 2, \dots, N$. Equation (7.1) computes the reorientation of the whole system. The first term of (7.1) is referred to as *dynamic phase* which will be zero if the system is originally at rest; the second term is referred to as *geometric phase* which will be of interest to us.

We now turn to systems of floating four-bar linkages. As we have seen, the riemannian metric given by \mathbf{J} in Section 4 is also invariant under the S^1 action. This implies that the formula (7.1) is applicable to floating four-bar linkages. We will consider Grashof and non-Grashof mechanisms separately.

Recall that, for Grashof mechanism, the configuration space (after center of mass reduction) is $S^1 \times S^1$, which can be parameterized by (θ_0, θ_1) globally. The corresponding shape space is simply S^1 . Recall that the angular momentum of the system is

$$\mu = (1, 1)\mathbf{J}\dot{\theta} \quad (7.2)$$

where $\dot{\theta} = (\dot{\theta}_0, \dot{\theta}_1)$. Since \mathbf{J} is a matrix of functions of $\theta_{10} \triangleq \phi$, one can derive the same equation as (7.1) with $N = 2$. By appealing to Proposition 4.3, one gets

$$\Delta\theta_0 = \int_0^T \frac{\mu}{\mathbf{e} \cdot \tilde{\mathbf{J}}\mathbf{e}} dt - \int_{\gamma} \frac{\mathbf{e} \cdot \tilde{\mathbf{J}}\tilde{\mathbf{M}}}{\mathbf{e} \cdot \tilde{\mathbf{J}}\mathbf{e}} d\theta_{10} \quad (7.3)$$

where $\mathbf{e} = (1, 1, 1, 1)^T$, $\tilde{\mathbf{J}}$ has been shown in Section 4 and $\tilde{\mathbf{M}}$ is the second column of $(I, \Omega^T)^T$ matrix, i.e.

$$\tilde{\mathbf{M}}^T = \left(0 \quad 1 \quad -\frac{l_1 \sin(\theta_3 - \theta_1)}{l_2 \sin(\theta_3 - \theta_2)} \quad \frac{l_1 \sin(\theta_2 - \theta_1)}{l_3 \sin(\theta_3 - \theta_2)} \right).$$

Recall that in Grashof case, the configuration space has two connected components, corresponding to leading form and lagging form, respectively. On these components, $\tilde{\mathbf{J}}$ has different symbolic expressions. Consequently, the phase shift generated by the same closed curve in shape space will be different. We illustrate this point by the following example.

Example 7.1:

Let $\mu = 0$. We choose the parameters as follows.

$$m_0 = 1, \quad m_1 = 1, \quad m_2 = 1, \quad m_3 = 1;$$

$$\begin{aligned}
I_0 &= 1, & I_1 &= 1, & I_2 &= 1, & I_3 &= 1; \\
\mathbf{d}_{03} &= (-1.5, 0), & \mathbf{d}_{01} &= (1.5, 0), & \mathbf{d}_{10} &= (-0.5, 0), & \mathbf{d}_{12} &= (0.5, 0), \\
\mathbf{d}_{21} &= (-1.5, 0), & \mathbf{d}_{23} &= (1.5, 0), & \mathbf{d}_{32} &= (-2, -1), & \mathbf{d}_{30} &= (2, -1).
\end{aligned}$$

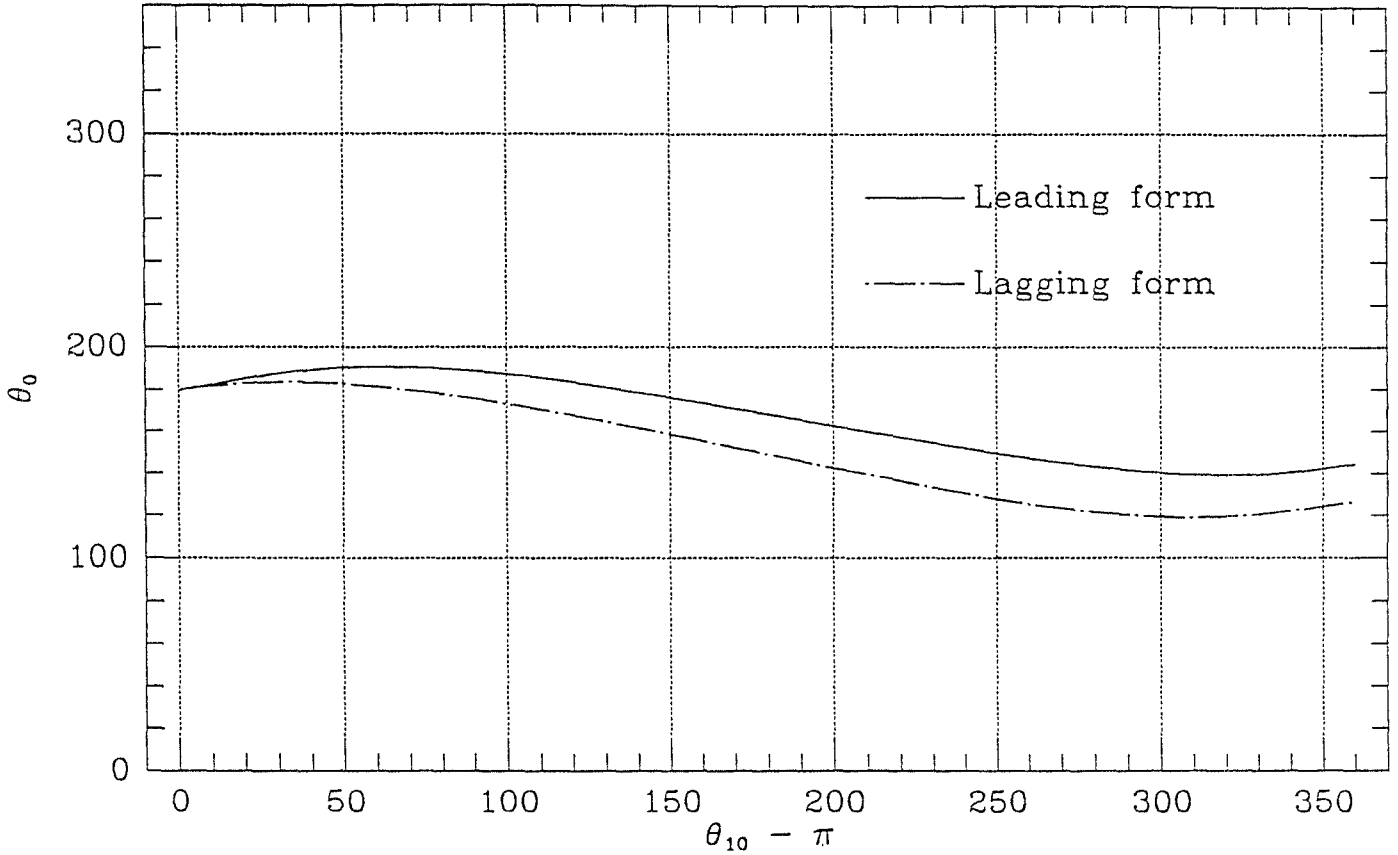


Figure 7.1

Figure 7.1 shows, for both leading and lagging form, how the orientation of the 0-th bar varies when the 1-st bar revolves about the 0-th bar. One can see that when the linkage returns to its original shape (in this example, the 0-th bar and 1-st bar are folded together), the 0-th bar has been re-oriented by $\Delta\theta_0$ which is less than zero. Its value for leading form is different from the one for lagging form because the existence of the mass-offset in the 3-rd bar. Here, we see again in Grashof mechanisms, two forms should be considered separately. ■

Now we consider non-Grashof mechanisms. Recall that in this case, the configuration space is still $S^1 \times S^1$ and the symmetry group is S^1 . However, the physical angles θ_0

and θ_1 cannot parameterize the configuration space globally. Nevertheless, the angular momentum of the system can still be expressed as (7.2) locally. More precisely, every element in the matrix \mathbf{J} is a branched function (branched by corresponding leading and lagging form) and not defined at the angle limits of θ_{10} . Since these limits are only two isolated points in shape space S^1 , the integration (7.3) can be performed. Let γ be the closed loop on S^1 given by

$$\gamma = \{\theta_{10}(t)|t \in \Delta_1\} \cup \{\theta_{10}(t)|t \in \Delta_2\} \triangleq \gamma_{lead} \cup \gamma_{lag}$$

where

$$\Delta_1 = \{t \in [0, T] | \sin(\theta_{32}) < 0 \text{ (leading form)}\}$$

$$\Delta_2 = \{t \in [0, T] | \sin(\theta_{32}) \geq 0 \text{ (lagging form)}\}$$

and $\Delta_1 \cup \Delta_2 = [0, T]$. Then the phase reconstruction (net reorientation) is given by

$$\Delta\theta_0 = \int_{\Delta_1} \frac{\mu}{\mathbf{e} \cdot \tilde{\mathbf{J}}\mathbf{e}} dt + \int_{\Delta_2} \frac{\mu}{\mathbf{e} \cdot \tilde{\mathbf{J}}\mathbf{e}} dt - \int_{\gamma_{lead}} \frac{\mathbf{e} \cdot \tilde{\mathbf{J}}\tilde{\mathbf{M}}}{\mathbf{e} \cdot \tilde{\mathbf{J}}\mathbf{e}} d\theta_{10} - \int_{\gamma_{lag}} \frac{\mathbf{e} \cdot \tilde{\mathbf{J}}\tilde{\mathbf{M}}}{\mathbf{e} \cdot \tilde{\mathbf{J}}\mathbf{e}} d\theta_{10} \quad (7.4)$$

In the following we show an example of the non-Grashof case.

Example 7.2:

Again, let $\mu = 0$. The parameters are given as follows.

$$m_0 = 5, \quad m_1 = 1, \quad m_2 = 1, \quad m_3 = 1;$$

$$I_0 = 5, \quad I_1 = 1, \quad I_2 = 1, \quad I_3 = 1;$$

$$\mathbf{d}_{03} = (-2, 0), \quad \mathbf{d}_{01} = (2, 0), \quad \mathbf{d}_{10} = (-1.5, 0), \quad \mathbf{d}_{12} = (1.5, 0),$$

$$\mathbf{d}_{21} = (-1.5, \lambda), \quad \mathbf{d}_{23} = (1.5, \lambda), \quad \mathbf{d}_{32} = (-1.5, 0), \quad \mathbf{d}_{30} = (1.5, 0).$$

It should be noted that this system has symmetric configurations for any λ . The scheme to change the shape of the system is given by the following steps.

1. Starting at a symmetry configuration in leading form;
2. Increasing $\theta_{10} - \pi$ until it reaches the dead point;
3. Decreasing $\theta_{10} - \pi$ in lagging form until it reaches the second dead point;
4. Increasing $\theta_{10} - \pi$ in leading form until it reaches the original symmetric configuration.

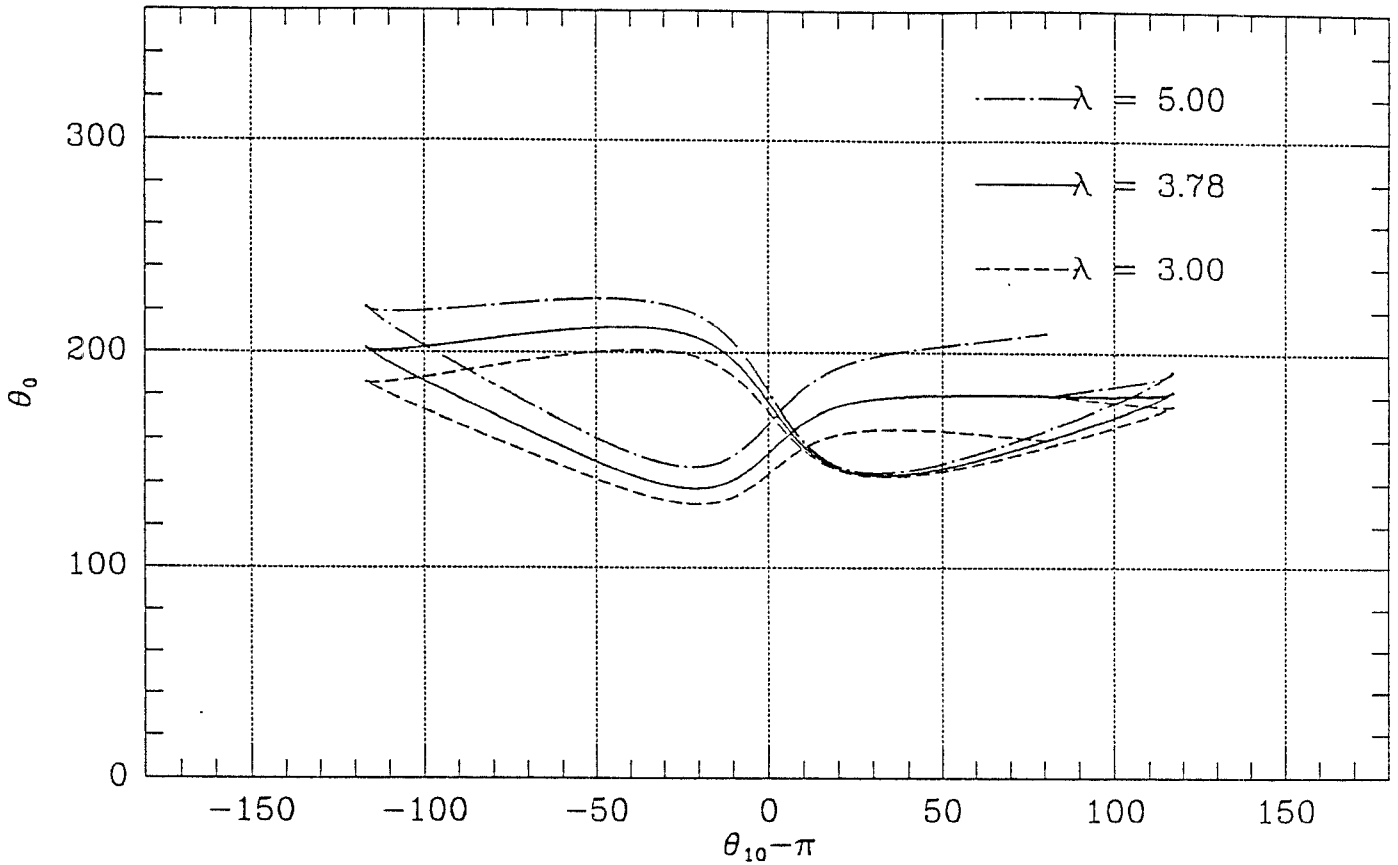


Figure 7.2

Figure 7.2 shows the change of θ_0 versus the change of the shape of the linkage by the above scheme for different λ . It is interesting to observe that the value for re-orientation of the 0-th bar can be positive, negative or zero. One can show that when a floating four-bar linkage is at rest at its symmetric configuration, varying the position of center of mass of the 0-th or the 2-nd bar so that the condition (6.6) is unchanged will not change the shape and the orientation of the system. Then, this example suggests that the system can be reoriented to arbitrary direction by allowing the center of mass of the 0-th or 2-nd bar to be movable so that the condition (6.6) is kept satisfied. ■

8. CONCLUSION

The kinematics and dynamics of planar, floating four-bar linkages have been investigated in this paper. We have observed that the topology of the configuration space for such linkages is related to the classical Grashof criterion. We have shown that, depending on the ratios of the lengths of the linkages, the configuration space is the union of two copies of $R^2 \times S^1 \times S^1$'s (Grashof mechanism), or a single copies of $R^2 \times S^1 \times S^1$ (non-Grashof mechanism), or $R^2 \times S^1 \times$ “figure 8” (change-point mechanism) which is not a smooth manifold. We have derived a closed form of the lagrangian for the system after accounting for the loop closure condition (potential energy has been ignored). The expression for the lagrangian reveals that systems of floating four-bar linkages possess S^1 symmetry after center of mass reduction. This property made it possible for us to understand the dynamics of the system via the theory of symplectic and Poisson reduction. Although the geometric structure of this system is parallel to that of the planar two-body problem (Sreenath et al. [1988]), because of the presence of kinematic loop constraints and greater freedom in the choice of structural parameters, floating four-bar linkages have more complicated and interesting dynamics. We have demonstrated this point by studying the relative equilibria for those linkages which admit symmetric configurations. As we have shown, a symmetric configuration is itself a relative equilibrium. If we vary certain kinematic parameters which preserve the symmetry, a symmetric relative equilibrium may be bifurcated. The type of bifurcations can be either supercritical or subcritical pitchfork. The stability of the relative equilibria at symmetric configurations was also investigated. The examples have shown that a floating four-bar linkage can have as many as ten relative equilibria. Finally, we investigated the re-orientation problem. We have shown that the formula for calculating the geometric phase for an open chain system can be extended to floating four-bar linkages. Through an example, we showed that for non-Grashof mechanisms which admit symmetric shape, the geometric phase shift may be generated in arbitrary direction.

As we have mentioned in the first section, a floating four-bar linkage is the simplest, but non-trivial multibody systems with closed loop. Fully understanding the kinematics and dynamics of these kinds of systems will certainly be useful in investigating more complicated systems. One can expect that the kinematic and dynamic properties of floating

four-bar linkages discovered in this paper will also show up in more complex systems. This will be pursued in future work.

Appendix A.

In this appendix, we review some basic concepts and results of bifurcation theory. The standard reference is (Golubitsky & Schaeffer [1985]).

Consider a single scalar equation

$$g(x, \lambda) = 0 \tag{A.1}$$

The bifurcation theory studies how the solutions x of this equation change with the parameter λ ; or, more precisely, what type of bifurcation occurs with parameter λ . Without loss of generality, one can assume $g(0, 0) = 0$. Moreover, we assume $g : R \times R \rightarrow R$ is smooth. This is one of the standard local (static) bifurcation problems with one state variable, called *the recognition problem*. As with many bifurcation problems, this problem can be solved successfully through singularity theory, in which the related issue is called *finite determinacy*. Let $z = (x, \lambda)$. Near origin, the function g can be written as

$$g(z) = \sum_{|\alpha| < k+1} \frac{1}{\alpha!} \left(\frac{\partial}{\partial z}\right)^\alpha g(0) z^\alpha + \sum_{|\alpha|=k+1} a_\alpha(z) z^\alpha, \tag{A.2}$$

for some smooth functions a_α defined in a neighborhood of the origin. Here we used the conventions with multi-indices:

$$\begin{aligned} |\alpha| &= \alpha_1 + \alpha_2, & \alpha! &= (\alpha_1)! (\alpha_2)!, \\ z^\alpha &= x^{\alpha_1} \lambda^{\alpha_2}, & \left(\frac{\partial}{\partial z}\right)^\alpha &= \left(\frac{\partial}{\partial x}\right)^{\alpha_1} \left(\frac{\partial}{\partial \lambda}\right)^{\alpha_2}. \end{aligned}$$

A key question is what terms in (A.2) can be ignored such that the values of coefficients of remaining terms can be used to determine the qualitative behavior of the original equation (A.1), for example, the variation in number of solutions. Singularity theory solves this problem by finding a suitable change of coordinates such that function g is equivalent to a standard model h , called *normal form*. A precise definition is given as follows (see (Golubitsky & Schaeffer [1985])).

Definition A.1: Two smooth mappings $g, h : R \times R \rightarrow R$ defined near the origin are *equivalent* if there exist a local diffeomorphism of R^2 , $(x, \lambda) \mapsto (X(x, \lambda), \Lambda(\lambda))$ at the origin and a nonzero function $S(x, \lambda)$, such that

$$g(x, \lambda) = S(x, \lambda) h(X(x, \lambda), \Lambda(\lambda)) \tag{A.3}$$

where $X_x(0,0) > 0$ and $\Lambda'(0) > 0$. If $\Lambda = \lambda$, g and h are *strongly equivalent*. ■

From this definition we see that, since $S(x, \lambda)$ is nonzero, the solution of $g(x, \lambda) = 0$ and $h(X, \Lambda) = 0$ are the same in the sense of diffeomorphism. From this point of view, by means of singularity theory one can show why and what the high-order terms in (A.2) do not effect the qualitative behavior of equation $g(x, \lambda) = 0$. It should be noticed that although this method does not tell us how to derive an appropriate normal form h , for most physical problems, such as the one considered in this paper, it is not hard to pick up some of the candidates from a large number of known simple polynomials of x and λ , or the model of normal forms which have standard bifurcation diagrams. This is in essence the spirit of application of singularity theory to a physical problem.

Without considering detailed issues of singularity theory which are applicable to bifurcation problems, we directly give the following result which will be used in the next section. For details see (Golubitsky & Schaeffer [1985]), chapter 2. First we need the concept of germs.

Definition A.2: Two smooth functions defined near the origin are *equivalent as germs* if there is some neighborhood of the origin on which they coincide. Let $\mathcal{E}_{x,\lambda}$ denote the set of equivalence classes of such functions. The elements in $\mathcal{E}_{x,\lambda}$ are called *germs*. ■

Lemma A.3: A germ $g \in \mathcal{E}_{x,\lambda}$ is strongly equivalent to

$$\epsilon x^k + \delta \lambda x \tag{A.4}$$

for $k > 2$ if and only if at $x = \lambda = 0$

$$g = \frac{\partial}{\partial x} g = \dots = \left(\frac{\partial}{\partial x}\right)^{k-1} g = \frac{\partial}{\partial \lambda} g = 0 \tag{A.5a}$$

and

$$\epsilon = \text{sgn}\left(\frac{\partial}{\partial x}\right)^k g, \quad \delta = \text{sgn}\frac{\partial}{\partial x} \frac{\partial}{\partial \lambda} g. \tag{A.5b}$$

Remark A.4: When $k = 3$ the normal form (A.4) provides a pitchfork bifurcation. From this lemma, so is g if (A.5) holds. It is easy to show that if $\epsilon\delta > 0$, the pitchfork bifurcation is subcritical; if $\epsilon\delta < 0$, the pitchfork bifurcation is supercritical. ■

Appendix B

The expression of ϵ_i and δ_i in the theorem 6.7 are of the following form.

$$\epsilon_1 = -12d_0^2(d_2 - d_0)^2(d_2^3 - d_0d_2^2 - d_0^2d_2 - 2d_2 + d_0^3 - 4d_0);$$

$$\epsilon_2 = 48d_0^2d_2((d_2 - d_0)^2 - 1)(d_2^2 - d_0^2)\sqrt{4 - (d_0 - d_2)^2};$$

$$\epsilon_3 = 48d_0^2d_2^2(d_2 - d_0)^2(d_2^3 - d_0d_2^2 - d_0^2d_2 - 4d_2 + d_0^3 - 2d_0);$$

$$\epsilon_4 = d_2^3((d_2 - d_0)^2 - 4)(d_2 - d_0)^2\sqrt{4 - (d_0 - d_2)^2};$$

$$\epsilon_5 = 2d_2^4((d_2 - d_0)^2 - 4)((d_2 - d_0)^3 - 4d_2).$$

Let

$$\Delta = 4d_2^2\sqrt{4 - (d_0 - d_2)^2}.$$

Then

$$\delta_1 = -\frac{1}{\Delta}(d_2 - d_0)^2\sqrt{4 - (d_0 - d_2)^2};$$

$$\delta_2 = -\frac{2}{\Delta}d_2(d_2^3 + 3d_0d_2^2 - 3d_0^2d_2 + 4d_2 + d_0^3).$$

References

- Abraham, R. & J. E. Marsden [1978], *Foundations of Mechanics* (Second edition), Revised, Enlarged, Reset, Benjamin/Cummings, Reading.
- Baillieul, J. [1988], "An enumerative theory of equilibrium rotations for planar kinematic chains," in *Dynamics and Control of Multibody Systems*, J. E. Marsden, P. S. Krishnaprasad & J. C. Simo, ed., Contemporary Math. #97, American Mathematical Society, 1-10.
- Baillieul, J. & M. Levi [1987], "Rotational Elastic Dynamics," *Physica D*, 27D.
- Bianchi, G. & W. Schielen [1985], "Dynamics of Multibody Systems," *Proceedings of IUTAM/IFTToMM Symposium*, Udine/Italy.
- Bloch, A. M., M. Reyhanoglu & N. H. McClamroch [1991], "Control and Stabilization of Nonholonomic Dynamic Systems," Preprint.
- CIME [1972], "Stereodynamics," edizione cremonese, Roma..
- Gibson, C. G. & P. E. Newstead [1986], "On the Geometry of the Planar 4-Bar Mechanism," *Acta Applicandae Math.* 7, 113-135.
- Golubitsky, M. & D. G. Schaeffer [1985], *Singularities and Groups in Bifurcation Theory, Volume I*, Springer-Verlag.
- Grashof, F. [1883], *Theoretische Maschinenlehre*, Verlag L. Voss, Leipzig.
- Grossman, R., P. S. Krishnaprasad & J. E. Marsden [1988], "The Dynamics of Two Coupled Three Dimensional Rigid Bodies," in *Dynamical Systems Approaches to Nonlinear Problems in Systems and Circuits*, F. Salam & M. Levi, eds., Philadelphia, 373-378 & SIAM Publ.
- Guillemin, V. & A. Pollack [1974], *Differential Topology*, Prentice-Hall, Inc., Englewood Cliffs, New Jersey.
- Hrones, J. A. & G. L. Nelson [1951], *Analysis of the four-bar linkage; its application to the synthesis of mechanisms*, The Technology Press of the Massachusetts Institute of Technology, and J. Wiley, & Sons, New York.

- Hunt, K. H. [1978], *Kinematic Geometry of Mechanisms*, Clarendon Press, Oxford.
- Krishnaprasad, P. S. [1990], "Geometric Phase, and Optimal Reconfiguration for Multibody Systems," *Proceedings of American Control Conference* 3, 2440–2444.
- Krishnaprasad, P. S. & J. E. Marsden [1987], "Hamiltonian Structures & Stability for Rigid Bodies with Flexible Attachments," *Arch. Rat. Mech. Anal.* 98.
- Krishnaprasad, P. S. & R. Yang [1991], "Geometric Phases, Anholonomy, and Optimal Movement," *Proceedings of the 1991 IEEE International Conference on Robotics and Automation* 3, 2185 – 2189.
- Krishnaprasad, P. S., R. Yang & W. Dayawansa, [1991], "Control Problems on Principal Bundles and Nonholonomic Mechanics," *Proceedings of 30th IEEE Conference on Decision and Control*, Brighton, England.
- Marsden, J. E., R. Montgomery & T. Ratiu [1990], "Reduction, symmetry, and phases in mechanics,," in *Memoirs of the AMS*.
- Marsden, J. E., P. S. Krishnaprasad & J. C. Simo, eds. [1988], *Dynamics and Control of Multibody Systems*, Contemporary Math. #97, American Mathematical Society.
- Oh, Y. G., N. Sreenath, P. S. Krishnaprasad & J. E. Marsden [1989], "The Dynamics of Coupled Planar Rigid Bodies Part II: Bifurcation, Periodic Orbits, and Chaos," *J. Dynamics & Differential Equations* 1, 269–298.
- Paul, B. [1979a], *Kinematics and Dynamics of Planar Machinery*, Prentice-Hall, Inc..
- [1979b], "A Reassessment of Grashof's Criterion," *Tran. of the ASME, J. of Mech. Design* Jul 101, 515–518.
- Posbergh, T. [1988], "Modeling and Control of Mixed and Flexible Structures," University of Maryland, College Park, Ph.D. Thesis, also, Systems Research Center Technical Report SRC TR88-58.

- Posbergh, T., P. S. Krishnaprasad & J. E. Marsden[1987], "Stability Analysis of a Rigid Body with a Flexible Attachment using the Energy-Casimir Method," in *Differential Geometry : The Interface between Pure and Applied Mathematics*, M. Luksic, C. F. Martin, W. Shadwick, eds., Contemporary Math. #68, 253–273., AMS & Providence.
- Shapere, A. [1989], "Gauge Mechanics of Deformable Bodies," University of California, Santa Barbara, Ph.D. Dissertation.
- Shapere, A. & F. Wilczek, eds. [1989], *Geometric Phases in Physics*, Advanced Series in Mathematical Physics #5, World Scientific.
- Simo, J. C., J. E. Marsden & P. S. Krishnaprasad[1988], "The Hamiltonian Structure of Nonlinear Elasticity: The Material and Convective Representation of Rods, Plates and Shells," *Arch. Rat. Mech. & Anal.* 104, 125–183.
- Simo, J. C., T. Posbergh & J. E. Marsden[1989], *Nonlinear Stability of Geometrically Exact Rods by the Energy-Momentum Method*, Stanford University, Division of Applied Mechanics., preprint.
- Smale, S. [1970], "Topology and Mechanics, I, II," *Invent. Math.* 11, 45–64.
- Sreenath, N. [1987], "Modeling and Control of Multibody Systems," University of Maryland, College Park, Ph.D. Thesis, also, Systems Research Center Technical Report *SRC TR87-163*.
- [1990], "Nonlinear Control of Multibody Systems in Shape Space," *Proceedings of the 1991 IEEE International Conference on Robotics and Automation* 3, 1776–1781.
- Sreenath, N., Y. G. Oh, P. S. Krishnaprasad & J. E. Marsden[1988], "The Dynamics of Coupled Planar Rigid Bodies Part I: Reduction, Equilibria & Stability," in *Dynamics & Stability of Systems* 3 #1&2, 25–49.
- Wang, L-S. & P. S. Krishnaprasad[1989], "Relative Equilibria of Two Rigid Bodies connected by a Ball-in-Socket Joint," *Proceedings of the IEEE Conference on Decision and Control* 2, 692–697.

Wittenburg, J. [1977], *Dynamics of Multibody Systems*, B.G. Teubner, Stuttgart.

Yang, R. & P. S. Krishnaprasad [1989], "On the Dynamics of Floating Four-bar Linkages,"
Proc. of the IEEE Conference on Decision and Control 2, 1632–1635.

_____ [1990], "On the Dynamics of Floating Four-bar Linkages II – Bifurcations
of Relative Equilibria," *Proceedings of 29th IEEE Conference on Decision and
Control* 3, 1288 – 1293.

